Universidade Federal do Rio de Janeiro

DIRECT-WRITE ASSEMBLY OF 3D SCAFFOLDS USING BETA-TRICALCIUM PHOSPHATES INKS FOR BONE REGENERATION

Raquel Costa Richard

2013

DIRECT-WRITE ASSEMBLY OF 3D SCAFFOLDS USING BETA-TRICALCIUM PHOSPHATES INKS FOR BONE REGENERATION

Raquel Costa Richard

Tese de Doutorado apresentada ao Programa de Pós-graduação em Engenharia Metalúrgica e de Materiais, COPPE, da Universidade Federal do Rio de Janeiro, como parte dos requisitos necessários à obtenção do título de Doutor em Engenharia Metalúrgica e de Materiais.

Orientadores: Rossana Mara da Silva Moreira Thiré
Gloria Dulce de Almeida Soares

Rio de Janeiro
Dezembro de 2013

DIRECT-WRITE ASSEMBLY OF 3D SCAFFOLDS USING
BETA-TRICALCIUM PHOSPHATES INKS FOR BONE REGENERATION

Raquel Costa Richard

TESE SUBMETIDA AO CORPO DOCENTE DO INSTITUTO ALBERTO LUIZ COIMBRA DE PÓS-GRADUAÇÃO E PESQUISA DE ENGENHARIA (COPPE) DA UNIVERSIDADE FEDERAL DO RIO DE JANEIRO COMO PARTE DOS REQUISITOS NECESSÁRIOS PARA A OBTENÇÃO DO GRAU DE DOUTOR EM CIÊNCIAS EM ENGENHARIA METALÚRGICA E DE MATERIAIS.

Examinada por:

_____

Profª. Rossana Mara da Silva Moreira Thiré, D.Sc.

_____

Profª. Gloria Dulce de Almeida Soares, D.Sc.

_____

Prof. Luiz Carlos Pereira, D.Sc.

_____

Dr. Jorge Vicente Lopes da Silva, D.Sc.

_____

Prof. Marcos Farina de Souza, D.Sc.

RIO DE JANEIRO, RJ - BRASIL
DEZEMBRO DE 2013

Richard, Raquel Costa

Direct-write assembly of 3D scaffolds using beta-tricalcium phosphates inks for Bone Regeneration/ Raquel Costa Richard. – Rio de Janeiro: UFRJ/COPPE, 2013.

XV, 60 p.: il.; 29,7cm.

Orientadores: Rossana Mara da Silva Moreira Thiré/ Gloria Dulce de Almeida Soares

Tese (doutorado) – UFRJ/ COPPE/ Programa de Engenharia Metalúrgica e de Materiais, 2013.

Referências Bibliográficas: p. 54-60.

1. Arcabouços ósseos. 2. Hidrólise de fosfatos de cálcio. 3. Substituição por magnésio. 4. Impressão 3D. 5. Engenharia de tecidos ósseos. I. Thiré, Rossana Mara da Silva Moreira *et al.* II. Universidade Federal do Rio de Janeiro, COPPE, Programa de Engenharia Metalúrgica e de Materiais. III. Título.

DEDICATION

I dedicate this thesis to Tsuneharu Ogasawara (*in memoriam)*, a man of boundless generosity who overlooked my background in dentistry and encouraged me towards the engineering field.

ACKNOWLEDGMENTS

My deepest gratitude goes to God. I might not know what my future holds, but walking with You, God, has given me faith, strength and perseverance. “For truly, I say to you, if you have faith like a grain of mustard seed, you will say to this mountain, ‘Move from here to there’, and it will move, and nothing will be impossible for you” (Matthew 17:20 ESV).

I owe a special thanks to my husband, Jim Richard, for his love and courage to embark in this journey with me.

I would like to show gratitude to all my lab colleagues. Thanks Marianna Oliveira, Ana Paula Duarte and Felipe Alencastro, for your help and collaboration. My special thanks goes to Renata Oliveira and Márcia Sader for all the time and effort to help me out; and for demonstrating that family is not always the people that have the same blood running through their veins.

I’m indebted to Dr. Racquel LeGeros (*in memorian*) for her supervision and advice at the Calcium Phosphate Research Laboratory (NYUCD). Without her it would be impossible to achieve the synthesis results.

I’m also grateful to: Dindo Mirajes, for all the laboratory training at the Department of Biomaterials and Biomimetics, New York University; Mary Walczak for her friendship and support; and Stephanie Ishack for guiding my firsts steps with the robocasting machine, for being available whenever I needed her help and for all the laughter that we had shared.

I thank Inayá Lima, from the Nuclear Instrumentation Laboratory (UFRJ), for the micro-CT analyses.

I would like to express my appreciation to all the technicians involved in this work.

I acknowledge the financial support given by CNPq, CAPES, FAPERJ.

Lastly but not least, I want to thank my mentors:

Gloria Soares, thank you for giving me the opportunity to be part of the Biomaterials Laboratory, for all your support, advice and patience through the difficult times. Thank you for being not only a professor but a role model for me.

Rossana Thiré, thank you for accepting me as your PhD student, for your understanding and assistance.

Resumo da Tese apresentada à COPPE/UFRJ como parte dos requisitos necessários para a obtenção do grau de Doutor em Ciências (DSc.)

CONSTRUÇÃO DE ARCABOUÇOS 3D PARA REGENERAÇÃO ÓSSEA USANDO MONTAGEM POR ESCRITA DIRETA COM TINTAS DE BETA-FOSFATO TRICÁLCICO

Raquel Costa Richard

Dezembro/ 2013

Orientadores: Rossana Mara da Silva Moreira Thiré
Gloria Dulce de Almeida Soares

Programa: Engenharia Metalúrgica e de Materiais

Várias técnicas têm sido desenvolvidas para reparo de perdas ósseas extensas, no entanto cada uma delas têm suas limitações. Atualmente, técnicas de manufatura aditiva têm demonstrado um grande potencial para uso em engenharia de tecidos ósseos. O objetivo do presente estudo foi sintetizar beta-fostato de cálcio (β-TCP), beta-fosfato de cálcio substituído por magnésio (β-TCMP) e fosfato de cálcio bifásico substituído por magnésio (BCMP) por meio de hidrólise e produzir arcabouços para regeneração óssea usando a tecnologia de *robocasting*. Pós de apatitas cálcio deficientes, com e sem magnésio, foram obtidas por hidrólise, calcinadas e físico-quimicamente caracterizadas. Teste colorimétrico de viabilidade celular, formação de nódulos de cálcio e a expressão de fosfatase alcalina, osteocalcina, fator de transformação do crescimento beta-1 e colágeno foram avaliados usando uma linhagem de células osteoblásticas de rato (MC3T3-E1). De acordo com o teste de viabilidade celular, os pós induziram proliferação celular. A formação de nódulos de cálcio e a atividade de marcadores ósseos sugeriram que os materiais apresentam potencial para engenharia de tecidos ósseos. Montagem por escrita direta de arcabouços cilíndricos periódicos foi realizada por deposição robótica usando tintas coloidais de β-TCP, β-TCMP e BCMP. Os arcabouços sinterizados foram caracterizados por difração de raios-x, Espectroscopia no infravermelho por transformada de Fourier, microscopia eletrônica de varredura, método de Arqumiedes e teste de compressão uniaxial. Os arcabouços constuídos por *robocasting* apresentaram poros interconectados e uma média de resistência à compressão entre 7.6 e 18.7 MPA, compatível com osso esponjoso.

Abstract of Thesis presented to COPPE/UFRJ as a partial fulfillment of the requirements for the degree of Doctor of Science (D.Sc.)

DIRECT-WRITE ASSEMBLY OF 3D SCAFFOLDS USING
BETA-TRICALCIUM PHOSPHATES INKS FOR BONE REGENERATION

Raquel Costa Richard

December/ 2013

Advisors: Rossana Mara da Silva Moreira Thiré
Gloria Dulce de Almeida Soares

Department: Metallurgical and Materials Engineering

Several approaches have attempted to replace extensive bone loss, but each of them has their limitation. Nowadays, additive manufacture techniques have shown great potential for bone engineering. The objective of the present study was to synthesize beta tricalcium phosphate (β-TCP), beta tricalcium phosphate substituted by magnesium (β-TCMP) and biphasic calcium phosphate substituted by magnesium (BCMP) via hydrolysis and produce scaffolds for bone regeneration using robocasting technology. Calcium deficient apatites powders, with and without magnesium, were obtained by hydrolysis, calcined and physico-chemically characterized. Colorimetric cell viability assay, calcium nodule formation and the expression of alkaline phosphatase, osteocalcin, transforming growth factor beta-1 and collagen were assessed using a mouse osteoblastic cell line (MC3T3-E1). According to the cell viability assay, the powders induced cell proliferation. Calcium nodule formation and bone markers activity suggested that the materials present potential value in bone tissue engineering. Direct-write assembly of cylindrical periodic scaffolds was done via robotic deposition using β-TCP, β-TCMP and BCMP colloidal inks. The sintered scaffolds were characterized by X-ray diffraction, Fourier-transform infrared spectroscopy, scanning electron microscopy, Archimede's method and uniaxial compression test. The scaffolds built by robocasting presented interconnected porous and exhibited mean compressive strength between 7.6 and 18.7 MPa, compatible with trabecular bone.

TABLE OF CONTENTS

LIST OF FIGURES

LIST OF TABLES

ABREVIATIONS

3D- three-dimensional

ACP- amorphous calcium phosphate

ALP- alkaline phosphatase

BCMP- magnesium substituted biphasic calcium phosphate

BCP- biphasic calcium phosphate

BMP(s)- bone morphogenetic protein(s)

BV- bone volume

CAD- computer-aided design

CaO- calcium oxide

CaP(s)- calcium phosphate(s)

CDA(’s)- calcium deficient apatite(s)

CPGs- calcium phosphates glasses

CPP- calcium pyrophosphate

CT- computerized tomography

DCPA- monetite, dicalcium phosphate anhydrous

DCPD- brushite, dicalcium phosphate dehydrate

DMSO- dimethyl sulfoxide

F4M- hydroxypropyl methylcellulose

FBS- fetal bovine serum

FTIR- Fourier-transform infrared spectroscopy

HA- hydroxyapatite

Mg-CDA's- magnesium substituted CDA's

micro-CT- *micro* computed tomography

MRI- magnetic resonance imaging

MTT- methylthiazolyldiphenyl-tetrazolium bromide

NaOH- sodium hydroxide

NYUCD- New York University College of Dentistry

OCP- octacalcium phosphate

PBS- phosphate buffered saline

PEI- poly(ethlyenimine)

ROI- region of interest

SEM- scanning electron microscope

TCP- tricalcium phosphate

TGF-β1- transforming growth factor- beta 1

TH- threshold

VOI- volume of interest

XRD- x-ray diffraction

α-MEM- alpha modified minimum essential medium

α-TCP- α-tricalcium phosphate

β-TCMP- magnesium substituted beta-tricalcium phosphate

β-TCP- beta-tricalcium phosphate

CHAPTER 1

INTRODUCTION

Replacing extensive bone loss remains a challenge. Several techniques were developed in the past years to overcome this problem, but each of them has their own limitation. Autogenous bone grafts have not just morbidity associated, but limitation in the quality and quantity of bone available. Allografts have a significant incidence of postoperative infection as well as potential for disease transmission (SCHELLER *et al.*, 2009). Taking this in account, using synthetic bone graft materials to control the complications associated with the current techniques seems to be a powerful alternative.

Commercial synthetic calcium phosphate compounds used as bone graft materials include: hydroxyapatite (HA); tricalcium phosphate (TCP); and biphasic calcium phosphate (BCP). The last one consists of an intimate mixture of HA, $Ca_{10}(PO_4)_6(OH)_2$, and beta-tricalcium phosphate (β-TCP), $Ca_3(PO_4)_2$, in varying HA/β-TCP ratios (LEGEROS *et al.*, 2003). One attractive feature of BCP is that the preferential dissolution of β-TCP compared to HA allows controlling the bioactivity or biodegradation of the material by varying the HA/β-TCP ratio (GARRIDO *et al.*, 2011). Due to its instability in water, β-TCP cannot be precipitated using aqueous conditions (LEGEROS, 1991 and SADER *et al.*, 2009). β-TCP and BCP can be obtained from calcium deficient apatites (CDA's) sintered from 700 °C up to 1120 °C (ARAÚJO *et al.*, 2009 and LEGEROS *et al.*, 2003).

Synthetic CDA's can be prepared by precipitation or hydrolysis of non-apatitic calcium phosphates (LEGEROS *et al.*, 2003). Wet precipitation is largely employed but hydrolysis method has, as an advantage, a simple processing route. Hydrolysis method uses monetite ($CaHPO_4$, DCPA) or brushite ($CaHPO_4.2H_2O$, DCPD) as starting powders (LEE *et al.*, 2009 and LEGEROS,1991). Some parameters that should be controlled in those syntheses are: pH, temperature, aging time and the stoichiometry of the reaction precursors. Any variation in composition leads to the formation of phases as: calcium pyrophosphate ($Ca_2P_2O_7$, CPP) for Ca/P < 1.5; HA and β-TCP for 1.5 <

Ca/P < 1.67; and HA and calcium oxide (CaO) for Ca/P > 1.67 (DESTAINVILLE *et al.*, 2003).

Ionic substitutions, such as Mg-for-Ca, take place in biological apatites (DOROZHKIN, 2009, LEGEROS, 1991 and SADER *et al.*, 2009). Consequently, magnesium (Mg) is frequently incorporated in calcium phosphates and in composite materials as they are considered promising materials for bone engineering (SADER *et al.*, 2009, SCOTT *et al.*, 2011, TAMINI *et al.*, 2011). Mg is one of the most important ions present in biological hard tissue; it plays a significant role in bone growth, since it influences osteoblast and osteoclast activity (ARAÚJO *et al.*, 2009, BOANINI *et al.*, 2010). In addition, substituting Mg for Ca is known to stabilize β-TCP (ARAÚJO *et al.*, 2009, LEE & KUMTA, 2010, SADER *et al.*, 2009). In this case, Mg-containing TCP is called Mg-substituted whitlockite or β-TCMP, while the biphasic Mg-containing calcium phosphate is frequently called BCMP. Magnesium substituted apatites have been shown to stimulate adhesion and proliferation of osteoblast cells (SADER *et al.*, 2009). Magnesium substituted CDA's (Mg-CDA's) can also be synthesized by hydrolysis using magnesium acetate tetrahydrate ($Mg(C_2H_2O_2)_2).4H_2O$ as magnesium source.

Even though health bone is able to self-regenerate, this regeneration is limited to a gap of a few millimeters. Therefore, filling the bone defect with a porous scaffold helps to enhance bone regeneration since the scaffold serves as a template for cell ingrowth and interactions as well as for extracellular bone matrix formation (BUTSCHER *et al.*, 2011). Conventional scaffold fabrication methods such as gas foaming, salt leaching, fiber meshing and emulsification are widespread, but they cannot produce a scaffold with full control of geometrical parameters (e.g. pore size and interconnection, size and porosity) (BUTSCHER *et al.*, 2011 and MIRANDA *et al.*, 2007). It has been shown that three-dimensional (3D) scaffolds with interconnected macroporous, reproducing the shape of the patient's bone defect, help to improve the biocompatibility of the scaffolds after surgical procedure (UCHIDA *et al.*, 2008 AND LI *et al.*, 2011).

Additive manufacture techniques as 3D printing, laser sintering, stereolithography, fused-deposition-modeling and robocasting allow the fabrication of customized scaffolds with complex shapes and high reproducibility from a computer-aided design (CAD) model. The ability to build tridimensional scaffolds mimicking the micro and macrostructure of natural bone may represent a great approach for the fabrication of bone repair structures (MIRANDA *et al.*, 2007 and SIMON *et al.*, 2007).

Among the additive manufacture methods, robocasting is a technique that uses water-based inks, with minimal organic content, e.g. < 1 wt% (BUTSCHER *et al.*, 2011 and MIRANDA *et al.*, 2007). These inks must exhibit a well-controlled viscoelastic response to retain shape upon deposition, as well as a high colloid volume fraction to avoid shrinkage after assembly. Concentrated colloidal inks with the proper viscoelastic behavior play an important role in retaining shape upon deposition (SMAY *et al.*, 2002). Because of this, robocasting is a low-temperature additive manufacture technique which stands out due to the ability of building ceramic scaffolds without using a support structure or a sacrificial mold (BUTSCHER *et al.*, 2011 and MIRANDA *et al.*, 2007).

Synthetic calcium phosphates scaffolds, mimicking the bone macrostructure, built by robocasting may be a promising approach in the bone tissue engineering field. Therefore, the objective of this study was: to synthesize three different calcium phosphate-based powders (β-TCP, β-TCMP and BCMP); access their biocompatibility performing *in vitro* tests with MC3T3-E1 cell line; physico-chemically characterize and process the β-TCP, β-TCMP and BCMP powders as colloidal inks; examine their performance in a robocasting machine building scaffolds for bone regeneration; and, finally, analyze the scaffolds architecture and mechanical strength.

CHAPTER 2

LITERATURE REVIEW

2.1- BONE TISSUE

In order to build a bone scaffold that mimic the extracellular bone matrix, it's desirable to understand the chemical, mechanical and structural properties of bone (BUTSCHER *et al.* 2011). Therefore, the first section of this review it's committed to the comprehension of the bone structure.

Bone tissue has mechanical and metabolic functions; it is the main constituent of the adult skeleton; and it is a refined composite on different perspectives. On a macro observation, bone tissue consists of two main parts: an external dense compact bone (called cortical bone) and a porous core called cancellous or trabecular bone. The presence of trabecular bone reduces the weight of bone and provides a large bearing area. The combination of a dense outer shear stress-resisting shell and a cellular inner structure results in a low weight structure with excellent bending resistance. On a nanometer perspective, bone is essentially a composite formed from a combination of 70 % of calcium phosphate crystals and 20–30 % of collagen matrix with some water. The combination of an elastic collagen matrix with a hard and brittle calcium phosphate mineral in a complex architecture leads to extraordinary mechanical properties (BUTSCHER *et al.* 2011 and GIBSON *et al*., 2010). According to the literature the compressive strengths of cortical and cancellous bone are in the ranges 100–230 and 2–12 MPa, respectively (BUTSCHER *et al.* 2011, GIBSON E ASHBY, 1997, GIBSON *et al*., 2010, HOUMARD *et al.* 2013 and HUTMACHER *et al.* 2007).

The bone tissue is related to mechanical and metabolic functions of the skeleton. It provides support for the body; protects vital organs such as brain and heart; multiplies the forces produced during skeletal muscle contraction to transform them into corporal movements; bounds cavities containing bone marrow, where blood cells are formed; servers as a reservoir of ions, specially calcium and phosphate, to keep the

body fluids concentration in a constant level (DOBLARÉ *et al*., 2004, JUNQUEIRA E CARNEIRO, 2010).

Approximately 99 % of the body's calcium is stored in the skeleton in the form of hydroxyapatite crystals. Calcium ions are essential for the activity of several enzymes and proteins which mediate cells adhesion, cytoskeletal movements, membrane permeability as well as other cellular functions. There is a continuous interchange between blood and bone calcium, which leads to a fairly stable concentration of calcium in the blood (9- 10 mg/dL) and tissues (JUNQUEIRA E CARNEIRO, 2010).

Bone can be basically described as a specialized connective tissue made up of a calcified extracellular material, called bone matrix, and three major cell types (osteocytes, osteoblasts and osteoclasts) (JUNQUEIRA E CARNEIRO, 2010).

The inorganic component of the dry bone represents, approximately, 65 % of its weight and it's predominantly composed of calcium phosphates ions and other components as magnesium, sodium and potassium. The calcium and phosphorus ions are organized, in the inorganic component of the bone, as hydroxyapatite crystals ($Ca_{10}(PO_4)_6(OH)_2$), nevertheless the calcium can be also found in its amorphous form. The organic component of the bone corresponds to 35 % of the dry weight of the bone. It includes: osteoprogenitor cells; osteoblasts; osteocytes; osteoclasts; collagen fibers, especially type I collagen (95 %); proteoglycans; and glycoproteins (JUNQUEIRA E CARNEIRO, 2010).

Osteoprogenitor cells are originated from stem cells, they are also known as pre-osteoblasts cells because they have the capability of developing into osteoblasts. Osteoblasts synthesize and secrete the organic components of bone matrix (type I collagen, proteoglycans and glycoproteins) and are also connected to the deposition of inorganic components. When the osteoblasts are surrounded by the mineralized matrix they differentiate as osteocytes. Osteoclasts are multinucleated, giant cells associated with the resorption and remodeling of bone tissue (JUNQUEIRA E CARNEIRO, 2010).

On a macroscopic scale the bone can be described as a structure made up of an outer shell of compact bone also known as cortical; and a cellular inner structure called cancellous or trabecular bone (GIBSON E ASHBY, 1997, GIBSON *et al*., 2010). On a microscopic scale, bone tissue reveals two distinct organizations: lamellar and woven bone. Lamellar bone can be described as consisting of multiple layers of calcified matrix (3-7 μm thick). Whether cortical or trabecular, most bone in adults is

organized as lamellar bone. The woven bone is usually more immature than lamellar bone, it's non-lamellar and can be characterized by its random disposition of type I collagen fibers. It's also the first bone to appear in the embryonic development and in a fracture repair. Most of the woven bone tissue is replaced, in adults, by lamellar bone tissue (DOBLARÉ *et al*., 2004,).

Bone growth process involves partial resorption of the bone tissue previously formed and the deposition of new bone. The last one exceeds bone resorption, leading to a net increase in bone mass. Nonetheless, bone's shape is maintained while its mass increases (JUNQUEIRA E CARNEIRO, 2010).

Bone is constantly being remodeled throughout adult life, which results in the removal of old bone and its replacement by a new one. In general, during bone remodeling, the processes of bone resorption and formation are coordinate so that there is no net change in bone mass. In diseases such as osteoporosis, bone resorption exceeds bone formation, leading to a net decrease in bone mass (DOBLARÉ *et al*., 2004, EIJKEN, 2007).

Bone usually has a excellent capacity of repair because it is very vascularized and contains osteoprogenitor cells, however its regeneration is limited to a defect of a few milimiters (BUTSCHER *et al.* 2011).

Bone fracture causes blood vessels rupture, which leads to a local hemorrhage or hematoma. Macrophages are the cells responsible to remove the clotted blood and tissue debris originated after the bone fracture, while the osteoclasts resorb the matrix of the damaged bone. Bone repair process is a repetition of embryonic bone development. It involves regenerative events stimulated by the bone fracture. Cells present at the fracture proliferates and differentiate into osteogenic and chondrogenic cell lines. This event is followed by membranous and endochondral ossification, which leads to the fracture healing, i.e., fracture callus (JUNQUEIRA E CARNEIRO, 2010 AND NAKASE & YOSHIKAWA, 2006).

2.1.1- MECHANICAL BEHAVIOR OF TRABECULAR BONE

A better understanding of structure-property relationships allows the design of bone substitutes with similar properties to the bone that they are replacing. The cellular

structure of trabecular bone consists of an interconnected network of rods or plates and its typical relative density is between 0.05 and 0.7; consequently, bones with relative density smaller than 0.7 are classified as trabecular. Figure 1 displays a micro-computed tomography image showing the cellular structure of trabecular bone. Trabecular bone has an optimized structural anisotropy due to the trabecular orientation along the principal stress trajectories (GIBSON E ASHBY, 1997, GIBSON *et al*., 2010).

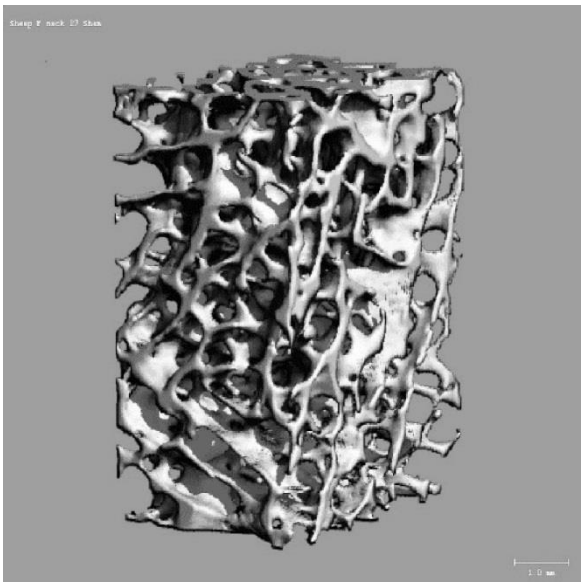

Figure 2.1: Micro-computed tomography image showing the cellular structure of trabecular bone (courtesy of Dindo Mirajes, NYUCD).

Since most of trabecular architectures are foam-like structures, bending and buckling are known as the primary mechanisms of deformation and failure for trabecular bone submitted to compression tests. Usually, trabecular bone deforms linearly elastically by bending and collapses, in compression, by inelastic buckling. Because some trabecular bone architectures are extremely aligned, probably as a result of loading being concentrated in on direction, they can deform in linear elastic regime by axial shortening rather than bending. They also may fail buckling or yielding (if dense enough). This produces a linear dependence of strength on density. Statistical analysis based on data available in the literature concluded that compressive strength of trabecular bone is proportional to density squared (GIBSON E ASHBY, 1997, GIBSON *et al*., 2010).

The spread in the mechanical properties data from trabecular bone is large due to its anisotropy, differences in its porosity and inorganic content (GIBSON *et al*., 2010). Table 1 shows the compressive mechanical properties and porosity of human bone (JOHNSON & HERSCHLER, 2011).

Table 2.1: Compressive mechanical properties and porosity of human bone. Adapted from (JOHNSON & HERSCHLER, 2011).

	Compressive strength (MPa)	**Porosity (%)**
Cancellous bone	4-12	30-90

2.2- TISSUE ENGINEERING

According to LANGER and VACANTI (1993) tissue engineering applies biology and engineering principles to the development of functional substitutes for injured tissue. These bio-substitutes should restore, maintain, or improve the morphology and functions of damaged tissues or organs. In this field, bone tissue engineering may be one of the first subdivisions of tissue engineering to experience successful clinical application.

2.2.1- BONE TISSUE ENGINEERING

Replacing or repairing bone defects caused by trauma, cancer, or congenital defects is a major clinical challenge. Thanks to its intrinsic osteoconductivity and osteoinductivity, autogenous bone grafting is the most popular clinical method used so far. Nonetheless, because it involves the removal of bone from the patient and transplantation into his bone defect, this procedure is limited by the amount of healthy bone that can be removed from the patient's donor site. Moreover, another disadvantage is the morbidity associated with the technique. Allogenic (from other

humans) and xenogenic (from non-human species) bones can be used as an alternative for autogenous bone; however the rejection is a risk that cannot be ignored. In addition, xenogenic bone has a significant potential for zoonotic disease transmission (HORNER *et* al., 2010 and SCHELLER *et al*., 2009). Due to these restrictions, the use of additive manufacture techniques for building bone scaffolds with synthetic materials has been receiving greater interest as they are considered substitutes for autografts, allografts and xenografts (HORNER *et* al., 2010 and ROY *et al.*, 2003).

Additive manufacture techniques as 3D printing, laser sintering, stereolithography, fused deposition modeling and robocasting, involve building customized scaffolds with complex shapes and high reproducibility from a computer-aided design (CAD) model. These techniques employ biocompatible polymers, hydroxyapatite and/or calcium phosphates to fabricate scaffolds, avoiding issues as rejection and limited donor site. An additional advantage of those techniques is the use of data obtained from computerized tomography (CT) or magnetic resonance imaging (MRI) medical scans to create a CAD model that will match the patient's bone defect. (BUTSCHER *et al.*, 2011, MIRANDA *et al.*, 2006 and MIRANDA *et al.*, 2007a).

3D biodegradable scaffolds, employed as templates for initial cell attachment and subsequent tissue regeneration, are essential for the success of bone tissue engineering. Because there are anatomical variances among patients and differences in bone defect, bone tissue engineering scaffolds should be customized to meet each patient needs. It has been shown that fabricating scaffolds according to the 3D shape of the patient's bone defect improves the biocompatibility of the implanted scaffold (UCHIDA *et al.*, 2008 and LI *et al.*, 2011).

2.2.1.1- SCAFFOLDS ENGINEERING

According to DETSCH *et al.* (2011) the scaffold is a crucial component in bone regeneration because it serves as a template for cell ingrowth/interactions and the formation of extracellular bone matrix to offer structural support to the newly formed tissue. In other words, it isn't just a passive component in bone tissue engineering, because it guides cell and tissue ingrowth by balancing the degradation of the scaffold to the tissue regeneration (BUTSCHER *et al.* 2011).

An ideal bone scaffold should match the complexity of bone properties. In order to achieve this goal the first step is to find a biocompatible material with desirable mechanical properties. So far, no artificial bulk material was able to mimic the bone perfect balance between elasticity, strength and fracture toughness. Based on this argument, cellular materials seem to be a promising approach for bone and scaffold engineering (BUTSCHER *et al.*, 2011 and GIBSON *et al*., 2010). A second step to achieve an ideal bone scaffold is to build up complex 3D structures which reproduce the bone architecture with precise resolution. The last step is to improve its mechanical properties (BUTSCHER *et al.* 2011).

As stated by HUTMACHER *et al.* (2000), a scaffold should have the following characteristics: biocompatibility and bioresorbability with a controllable degradation and resorption rate which matches cell/tissue growth in vitro and/or in vivo; appropriate surface chemistry for cell attachment, proliferation and differentiation; three-dimensional geometry and interconnected porous network for cell growth, flow transport of nutrients and metabolic waste; and mechanical properties similar to those of the tissues at the site of implantation. XIE *et al.* (2006) stated that an ideal scaffold should also be capable of delivering growth factors with temporal and spatial control in order to promote cellular development and morphogenesis. Furthermore, SCHELLER *et al.* (2009) suggested that an ideal bone substitute should have the biological advantages of an autograft and supply advantages of an allograft. At the same time they acknowledge that is difficult to assimilate high porosity and mechanical integrity into a single material design, as mechanical properties are frequently maximized by minimizing porosity (SCHELLER, *et al*., 2009). For DETSCH *et al.* (2011), a bone scaffold should have porosity of 30–70 vol% and a pore diameter between 300 and 800 μm so that could allow bone ingrowth. The authors disclose that the bone substitute strength should be between 0.5 and 15 MPa, considering a cancellous bone replacement. In other words, the bone substitute strength should be similar of the bone to be replaced. For REZWAN *et al.* 2006, a scaffold with satisfactory mechanical strength shouldn't collapse during handling and during the patient's normal activities. In addition some authors state that the scaffold strength should be bigger than the bone strength in the defect site (BABIS & SOUCACOS, 2005).

As exposed above, the mechanical properties goal for bone scaffolds is diverse. Nevertheless, an important fact to be considered is that the initial mechanical properties of the material employed to build the scaffold should account both the properties changes with degradation and the expected bone in-growth. For instance,

polymers degradation rates can vary from days to months while degradation rates for calcium phosphates can vary from months to years. (JOHNSON & HERSCHLER, 2011).

2.2.1.2- CALCIUM PHOSPHATES

Bone substitute biomaterials are required to build custom-made scaffolds via additive manufacture. Besides many organic and inorganic materials, calcium phosphate (CaP) compositions play an important role in this field. For instance, materials like hydroxyapatite (HA), tricalcium phosphate (TCP) and biphasic calcium phosphates (BCP) are employed to assembly 3D bone scaffolds due to their similarity in composition with the inorganic phase of hard tissues (DETSCH *et al.*, 2011, LEGEROS, 1991 and SADER *et al.*, 2013). Besides their similarity in composition to the bone mineral phases, they have some similarities related to bone properties as: biodegradability, bioactivity, and osteoconductivity (LEGEROS, 2008). But, in spite of these desirable properties, one of the limiting factors for the use of calcium phosphates in load-bearing applications is strength, due to the inherent brittleness of this class of materials (JOHNSON & HERSCHLER, 2011).

Some calcium phosphates materials including porous synthetic HA, coralline HA, β-TCP, porous BCP, calcium phosphate cements and OCP (octacalcium phosphate) coatings on Ti alloy have been reported to be osteoindutive, as they induced bone formation without the presence of osteogenic factors. Because this osteoinductive property was observed in some CaP materials but not in others with similar composition, those materials were described to have “intrinsic” osteoinductivity. This phenomenon was attributed to the topography, geometry, macropore size, and porosity of the CaP, since these features could allow confinement and concentration of circulating bone growth factors (BMPs) and osteoprogenitor cells into the CaP materials (LEGEROS, 2008).

CaPs have a high affinity for growth factors such as BMP-2, which stimulates proliferation and differentiation of osteoprogenitor cells. Consequently, CaPs are appropriate carriers for growth factors and stem cells, not requiring chemical surface modification as some polymers do. Their dissolution process is followed by reprecipitation of a carbonated apatite, which has composition and chemical structure

similar to the mineral phase of the bone. Lastly, the degradation rate of CaPs is slower than that of many polymers and associated with bone growth (JOHNSON & HERSCHLER, 2011).

Due to the characteristics listed above, HA, β-TCP and BCP are widely used in bone repair. Among these, HA has been used in bone cements for the repair of craniofacial defects, for maxillary sinus floor augmentation and in coatings for hip replacements. β-TCP ceramics have been employed as bioresorbable synthetic bone substitutes and are used in orthopedic and dental applications. Aside from the mechanical properties, the main difference between the properties of HA and β-TCP is their relative dissolution rates; HA is considered a more stable phase while β-TCP is a more soluble one. Thus, the use of BCP with different HA/ β-TCP ratios allows to manipulate dissolution rate and to obtain different mechanical properties (JOHNSON & HERSCHLER, 2011, LEGEROS, 2008 and GARRIDO *et al.*, 2011).

Calcium phosphate ceramics as HA and TCP are well established as suitable materials for bone substitute implants. Because of its resorption characteristics TCP support the strategy of regenerative bone therapy. Meaning, TCP stimulates the self-healing process of the host bone by synchronizing its resorption and the regeneration of the native bone (QU *et al.*, 2004 and TADIC & EPPLE, 2004).

2.2.1.3- ROBOSCASTING

Robocasting, also referred to as direct-write assembly, consists in the robotic deposition of rods of ink (concentrated colloidal suspensions), capable of self-supporting their weight during assembly. The rods are deposited, following a computer-aided design (CAD) model, to build up a 3D structure. Additionally, if the CAD model is obtained from medical scan data as computerized tomography or nuclear magnetic resonance imaging, the scaffold's external shape can be assembled to match the critical bone defect. The use of water-based inks with a minimal organic content (<1 wt %) and the absence of sacrificial support material or mold is a remarkable feature of robocasting. Since the use of lager amounts of binders complicates the scaffold's sintering and densification processes, robocasting seems to be a very attractive technology for building ceramic scaffolds (MIRANDA *et al.*, 2006 and MIRANDA *et al.*, 2007b).

The robocasting technique uses an ink delivery system fixed on a z-axis motion platform for printing onto a moving x-y platform. The tree-axis motions are independently controlled by a CAD direct-write program which allows the construction of complex, 3D architectures in a layer-by layer deposition scheme. The ink is stored in a syringe and deposited through a cylindrical nozzle at a specific volumetric flow rate necessary to maintain a constant x-y table speed. The deposition is performed under a non-wetting oil to prevent drying and shrinkage during assembly (SMAY, *et al.* 2002b).

Direct-write assembly using concentrated colloidal suspensions offers a new approach for building 3D periodic calcium phosphates scaffolds. It allows outstanding control over structural features of 3D scaffolds as: rod dimensions; macro-pore dimensions between rods; surface roughness; and rods micro-porosity (MICHNA, *et al.*, 2005 and SIMON *et al.*, 2007).

2.2.1.3.1- INKS

Ink formulations as dispersed colloidal fluids, highly shear thinning colloidal suspensions, and colloid-filled organic inks have been explored over the past years. These inks are desirable for fillings spaces in solids, but they are not capable of supporting their own weight when employed in structures with high aspect ratio walls or unsupported elements. This happens because of their initial fluidity and issues associated with controlling drying kinetics in multilayer assembling. In order to have an ink composition with self-supporting features, two important criteria need to be fulfilled. The first one is a well-controlled viscoelastic response, which allows the ink to flow through the deposition nozzle and then dry immediately to preserve the shape designed (even when gaps are present in the previous layer). The second criterion is that those inks must contain a high colloid volume fraction to reduce drying-induced shrinkage after the assembly process (SMAY, *et al.* 2002a).

MICHNA *et al.* (2005) concluded, in their study, that concentrated HA inks require high solids loading (45 vol %) and high elastic shear modulus (10^5 Pa) to be considered appropriate for the direct-write assembly of 3D periodic scaffolds.

Colloidal gels involve of a network of attractive particles able to transmit stress above a critical volume fraction (ϕ_{gel}), known as gel point. Two parameters rule the

equilibrium mechanical properties of colloidal gels: ϕ (the colloid volume fraction), which is proportional to their bond density; and ϕ_{gel}, which is inversely proportional to the bond strength. Thus, colloidal gels (of constant ϕ) experience a substantial increase in their elastic properties, when the interparticle forces are more attractive (SMAY, *et al.* 2002b).

2.3- PREPARATION OF CALCIUM PHOSPHATES

Commercial calcium phosphates for bone repair include: CDA, when Ca/P molar ratio is less than the stoichiometric value of 1.67 for pure HA; HA; β-TCP; and BCP, which is an intimate mixture of either β-TCP and HA or α-TCP and HA. Substituted apatites, substituted tricalcium phosphates, calcium phosphate glasses (CPGs), and other calcium phosphates such as OCP are classified as experimental calcium phosphate-based biomaterials. CDA can be prepared by precipitation or hydrolysis of dicalcium phosphate dehydrate (DCPD or brushite, $CaHPO_4.2H_2O$) or dicalcium phosphate anhydrous (DCPA or monetite, $CaHPO_4$). HA can be obtained by precipitation, hydrolysis, or hydrothermal methods at high pH followed by sintering at 1000-1200 °C. BCP can be prepared by sintering CDA above 900 °C and the resulting HA/TCP weight ratio will be governed by the Ca/P ratio of the CDA before sintering. Finally, substituted apatites or substitutedTCPs can be synthesized by precipitation, hydrolysis, hydrothermal, or solid state reactions (DOROZHKIN, 2009, LEGEROS, 2008).

The preparation techniques of these calcium phosphates will be reviewed in the following subchapters.

2.3.1- β-TCP PREPARATION

Pure β-TCP cannot be obtained from aqueous systems, due to its instability in water. It is a high temperature phase, which can be prepared by: solid-state interaction of acidic calcium orthophosphates (e.g., dicalcium phosphate anhydrous), with a base (e.g., CaO) at a temperature of 800 to 1000 °C; or thermal decomposition of a CDA. In

addition to the chemical preparation routes, ion-substituted β-TCP can be prepared by calcining bones (DOROZHKIN, 2009, LEGEROS, 1991, SADER *et al.*, 2009).

β-TCP transforms into a high-temperature phase known as α-tricalcium phosphate (α-TCP) at temperatures above, approximately, 1125 ºC. The α-TCP phase is more soluble in water, at room temperature, than the β-TCP one (DOROZHKIN, 2009).

2.3.2- β-TCMP PREPARATION

Pure β-TCP never occurs in biological systems. The reason why is that β-TCP structure contains calcium ion vacancies which aren't big enough to accommodate others calcium ions, instead they allow the inclusion of magnesium ions. In addition, substituting Mg for Ca is known to stabilize β-TCP. Mg-containing TCP is called Mg-substituted whitlockite, β-TCMP or Mg-TCP; the biphasic Mg-containing calcium phosphate is frequently called BCMP or Mg-BCP (ARAÚJO *et al.*, 2009, DOROZHKIN, 2009, LEE & KUMTA, 2010, LEGEROS, 2008, SADER *et al.*, 2009).

β-TCMP can be synthesized from aqueous systems using solutions containing Mg, with Mg/Ca molar ratio from 0.25 to 0.5 via: precipitation; hydrolysis of DCPD, at a temperature of 60 °C; or hydrolysis of DCPA, at 95-100 °C. It is important to remember that DCPD, frequently, partially converts to DCPA in dry storage. Additionally, β-TCMP can be prepared by solid-state reactions conduced at temperatures above 800 °C and can be possibly grown in gel systems (LEGEROS, 1991).

2.3.3- CALCIUM HYDROXYAPATITES PREPARATION

Pure HA, as well as pure β-TCP, cannot be obtained from aqueous systems, but it can be synthesized by:

1) precipitation followed by sintering- HA can be made when apatites are precipitated from solution with pH> 11 and then sintered at a temperature above 900 °C;

2) precipitation, with long digestion time, at 70 °C or 100 °C;
3) hydrothermal methods- at 375 °C;
4) and solid-state diffusion methods- at temperatures above 900 °C, e.g., by the reaction of $CaCO_3$ and $Ca(H_2PO_4)_2.H_2O$ with a Ca/P ratio of 1.67 at 1200 °C (LEGEROS, 1991).

Calcium-deficient apatites (CDA's), which are apatites with Ca/P molar ratio smaller than 1.67 (i.e., nonstoichiometric), can be prepared from aqueous systems via precipitation or hydrolysis if the initial pH of the solution is lower than 12 and the temperature range is between 25-100 °C. When the precipitation method is the choice, the lower the pH of the initial solution, the higher will be the temperature required for obtaining the apatite. If low temperatures and low pH are combined, it leads to non-apatitic calcium phosphates (e.g. DCPD) or OCP formation. Another feature related to the pH is the crystallinity of the CDA obtained at 80-100 °C. Meaning: the lower the pH the higher the crystallinity. In order to prepare CDA by hydrolysis, non-apatitic calcium phosphates as: amorphous calcium phosphate (ACP); DCPD; DCPA; OCP; or β-TCP can be used as starting powders (LEGEROS, 1991, LEGEROS *et al.*, 2003).

2.3.4- BIPHASIC CALCIUM PHOSPHATES PREPARATION

The intimate mixture of HA and β-TCP forms a biphasic calcium phosphate (BCP) which is widely used as a bone substitute bioceramic. BCP is obtained after sintering calcium-deficient biologic or synthetic apatites (prepared by precipitation or hydrolysis) at 700 °C or above (LEGEROS *et al.*, 2003). The equation below summarizes the reaction:

$$Ca_{10-x}M_x(PO_4)_{6-y}(HPO_4)_y(OH)_2 \rightarrow Ca_{10}(PO_4)_6(OH)_2 + Ca_3(PO_4)_2$$

CDA HA β-TCP

The HA/β-TCP ratio of the BCP can vary depending on the calcium deficiency of the unsintered apatite and/or sintering temperature. On the other hand, during the

hydrolysis of DCPD in sodium hydroxide (NaOH) solution, the calcium deficiency of the unsintered apatite can be controlled by the concentration of NaOH solution and by the ratio of weight of the DCPD to the total volume of the solution. Moreover, when hydrolysis of DCPD is performed in phosphate solution it results in apatite with bigger calcium deficiency (LEGEROS *et al.*, 2003).

CHAPTER 3

OBJECTIVE AND SPECIFIC AIMS

3.1- OBJECTIVE

The tissue engineering field needs to be further explored and has great potential for application in life sciences. Therefore, in this research, β-TCP, β-TCMP and BCMP powders were synthesized and processed into colloidal inks in order to build scaffolds for bone tissue engineering application using an additive manufacture method known as robocasting.

3.2- SPECIFIC AIMS:

- Synthesize β-TCP, β-TCMP and BCMP calcium phosphate powders via hydrolysis and characterize them by physico-chemical and *in vitro* biological means;
- Develop β-TCP, β-TCMP and BCMP colloidal inks for *robocasting* (also known as *direct-write assembly* or robotic deposition) of 3D periodic scaffolds;
- Produce β-TCP, β-TCMP and BCMP scaffolds by robocasting.

CHAPTER 4

MATERIAL AND METHODS

4.1- STUDY GROUPS

Three groups of 3D calcium phosphates scaffolds were fabricated using an additive manufacture method known as robocasting. Each group was prepared with distinct calcium phosphate composition: β-TCP; β-TMCP; and BCMP, which consisted of an intimate mixture of HA and β-TMCP in a ratio of, approximately, 51/50 % w/w (ratio obtained after calcination at 950 °C for 11h).

4.2- EXPERIMENTAL PROCEDURES

4.2.1- SYNTHESIS OF CALCIUM-DEFICIENT APATITES (CDA'S)

Mg-substituted and Mg-free CDA's were prepared by hydrolysis methods according to three different compositions, as shown in Table 4.1, in order to be transformed into β-TCP, β-TMCP, and BCMP after calcination (Richard, *et al.*, 2013). The synthesis process was conceived at the Calcium Phosphate Research Laboratory of New York University College of Dentistry (NYUCD), as part of this research, and supervised by Dr. Racquel Z. LeGeros.

Table 4.1: Calcium-deficient apatites compositions. For all compositions, 100 g of brushite ($CaHPO_4.2H_2O$) and 1 L of double-distilled water was employed.

Composition	**Calcium acetate monohydrate ($CaC_4H_6O_4.1H_2O$)**	**Magnesium acetate ($Mg(C_2H_3O_2)_2.4H_2O$)**
A	44.045g (0.25 M)	x
B	44.045g (0.25 M)	10.723g (0.05 M)
C	88.09g (0.5 M)	21.446g (0.1 M)

Composition A: 44.045 g (0.25 M) of calcium acetate monohydrate (CaC4H6O4.1H2O) was dissolved in 1 L of double distilled water.

Composition B: 10.723 g (0.05 M) of magnesium acetate ($Mg(C_2H_3O_2)2.4H_2O$) and 44.045g (0.25 M) of calcium acetate monohydrate ($CaC_4H_6O_4.1H_2O$) were dissolved in 1 L of double distilled water.

Composition C: 21.446 g (0.1 M) of magnesium acetate ($Mg(C_2H_3O_2)2.4H_2O$) and 88.09 g (0.5 M) of calcium acetate monohydrate ($CaC_4H_6O_4.1H_2O$) were dissolved in 1 L of double distilled water.

After this first step, 100 g of dibasic calcium phosphate dihydrate (CaHPO4.2H2O, DCPD or brushite) was dissolved into the solution. All reagents were purchased from Fisher Scientific, Fair Lawn, New Jersey. Once the brushite was completed dissolved, with the help of a magnetic stir bar, the pH was adjusted to 5 (composition A and B) and 9 (composition C), using sodium hydroxide (NaOH) 5M. A higher pH was necessary to obtain BCMP since HA phase is stabilized in a basic environment, i.e. pH ≥ 8 (RAYNAUD, *et al*, 2002). The solutions were aged, on a stirring hot plate, for 24 h at a temperature range of 90-100 ˚C. The Figure 4.1 shows three steps of the CDA's preparation.

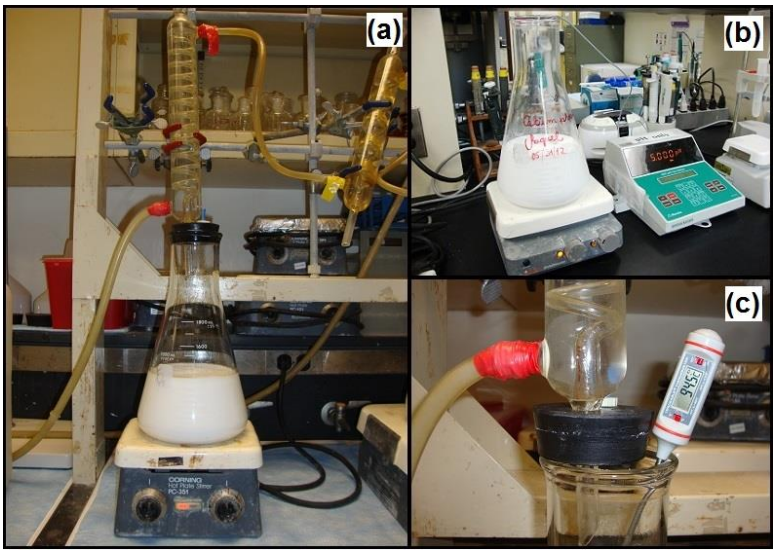

Figure 4.1: (a) brushite dissolution; (b) pH adjustment after brushite dissolution; and (c) temperature control during solution aging.

After being aged, the solutions were transferred to a stirring plate without heat and cooled down to room temperature. Then, the pH was adjusted to 7 with NaOH. The CDA's were filtered and washed using double distilled water. During the filtering process the pH was double checked to assure it was neutral. The CDA's were dried at 80 ˚C. The CDA's A, B and C were calcined at 950 ˚C to be transformed into β-TCP, β-TCMP and BCMP, respectively. The resulting powders were passed through a 100 mesh (150 μm) sieve.

4.2.2- CALCIUM PHOSPHATES POWDERS CHARACTERIZATION

4.2.2.1- X-RAY DIFFRACTION

X-ray diffraction is the most effective method for determining the crystal structure of materials, because it can identify chemical compounds from their crystalline structure and not from their chemical elements composition. Thus, the synthesized powders (β-TCP, β-TMCP, and BCMP), green and calcined, were characterized by X-ray diffraction (XRD) on a Shimadzu 6000 X-ray diffractometer,

using a CuKα radiation at 30 KV and 30 mA (2θ= 3-80°), in order to evaluate their crystallinity.

4.2.2.2- FOURIER-TRANSFORM INFRARED SPECTROSCOPY

Fourier-transform infrared spectroscopy (FTIR) is one of the vibrational spectroscopy techniques most commonly used by scientists and engineers to characterize materials. Therefore, the β-TCP, β-TMCP, and BCMP calcined powders were characterized by FTIR (Nicolet Magna-IR 550 Spectrometer Series II), recorded in the range of 4000 - 400 cm^{-1}, 64 scans and resolution of 4 cm^{-1} to identify their absorption bands.

4.2.2.3- INDUCED COUPLED PLASMA ATOMIC EMISSION SPECTROMETRY

The β-TCP, β-TMCP, and BCMP powders, calcined at 950 °C, were submitted to induced coupled plasma atomic emission spectroscopy (ICP) (Thermo Jarrell Ash, Trace Scan Advantage), where the specimen and standard solutions were pumped through argon plasma, which was excited by 2 kW/27.12 MHz radio frequency generator, to determine their calcium, phosphorus and magnesium concentrations.

The samples were prepared dissolving 10 mg of the respective powder with 10 drops of hydrochloric acid 17 %. This solution was transferred to a 100 ml volumetric flask and double distilled water was added up to the 100 ml mark of the volumetric flask.

4.2.2.4- PARTICLE SIZE AND DISTRIBUTION

In order to assess the particle size and distribution of the calcined β-TCP, β-TMCP, and BCMP powders, a Mastersizer 2000 (Malvern Instruments Ltd., Malvern,

UK) optical system for sizing materials in the range 0.02 to 2000 µm was employed. Additionally, the Hydro 2000MU sample dispersion unit was used, with water as dispersant agent.

4.2.2.5- SCANNING ELECTRON MICROSCOPE

Since the scanning electron microscope (SEM) is able to assess microscopic structures with high resolution and good depth of field, this technique was chosen to examine the morphology of the green and calcined β-TCP, β-TMCP, and BCMP powders. For this purpose a JEOL (JSM6460LV) was used working at 15 kV.

4.2.3- *IN VITRO* CHARACTERIZATION

Methylthiazolyldiphenyl-tetrazolium bromide (MTT) assay, mineralization assay and the expression of ALP, Osteocalcin, TGF-β1 and Collagen were performed aiming to assess the biocompatibility of the calcined powders as well as their potential to promote bone formation. In order to quantify the biodegradability of these materials a degradation test was performed.

4.2.3.1- MTT ASSAY

MTT assay was performed with MC3T3-E1 cell line (American Type Culture Colletion, 10801 University Boulevard, Manassas, VA 20110, USA) to determine the cytotoxicity of the calcined powders. In this assay 100 µL of $1x10^6$/ml cells were seeded in a 96 well plate, and cultured in alpha modified minimum essential medium (α-MEM), supplemented with 10 % of fetal bovine serum (FBS), for 24 h at 37 °C. Then, cells were exposed to β-TCP, β-TCMP and BCMP extracts in different concentrations for 24 h. β-TCP, β-TCMP and BCMP extracts were made from a stock solution (100 µg/µl in phosphate buffered saline, PBS) shaken overnight at room

temperature, then 25 µl were added into a specific amount of medium (α-MEM supplemented with 10 % of FBS) to achieve different final concentrations.

The concentrations of the extracts were the following:

BCMP (ug/ml): 50, 100 and 200 µg/ml

β-TCMP (ug/ml): 10, 20 and 40 µg/ml

β-TCP (ug/ml): 2.5, 5, 10, 20 and 40 µg/ml

Ten µL of MTT were added per well 4 h before ending the treatment. When purple precipitates were clearly visible under microscope, 100 µL of DMSO (dimethyl sulfoxide) were added to all wells to dissolve the formazan crystals. The absorbance of this colored solution was quantified by a spectrophotometer at a 570 nm wavelength.

4.2.3.2- MINERALIZATION ASSAY

Mineralization was assessed as a function of osteogenic behavior of β-TCP, β-TCMP and BCMP powders in MC3T3-E1 cell line. The cells were plated in 12-well tissue culture plates at a density of 7.6 x 10^4 cells/ well. β-TCP, β-TCMP and BCMP extracts were made from a stock solution (100 µg/µl in phosphate buffered saline, PBS) shaken overnight at room temperature, then 25 µl were added into 50 ml of medium (α-MEM supplemented with 10 % of FBS) for a final concentration of 50 µl/ml. One ml of extract was placed in each culture plate well and the cells were cultured up to 21 days, with 3 time points (1, 2 and 3 weeks). The medium was changed every 3 days. Mineralized nodules were detected by staining the cells with 0.1 % Alizarin Red per 1 hour and subsequently staining with 0.1 % light green SF solution for 30 min. Before being observed by light microscopy, cells were serially washed with 1 % acetic acid (3 times) and absolute ethanol (2 times).

4.2.3.3- ENZYME-LINKED IMMUNOSORBANT ASSAY (ELISA)

The expression of bone formation markers (alkaline phosphatase, ALP; and osteocalcin) and bone resorption markers (transforming growth factor- beta 1, TGF-β1 and collagen) were assessed in MC3T3-E1 cell line using: SensoLyte® pNPP Alkaline Phosphatase Assay Kit (AnaSpec, Inc., Fremont, CA, USA); Mouse type I Collagen Detection Kit (Chondrex, Inc, Redmond, WA, USA); Mouse Osteocalcin EIA Kit (Biomedical Technologies, Inc, Stoughton, MA, USA); and Mouse TGFβ1 ELISA Kit (Insight Genomics, Fall Church, VA, USA), respectively, according to the manufacturer's instruction.

The cells were exposed to β-TCP, β-TCMP and BCMP extracts with a 50 µl/ml concentration. One ml of extract was placed in each culture plate well and the cells were cultured up to 21 days, with 3 time points (7, 14 and 21 days). PBS was employed at the control group, because it was also used to dissolve the calcium phosphates powders.

4.2.3.4- DEGRADATION TEST

In order to quantify the biodegradability of β-TCP, β-TCMP and BCMP powders, the ISO 10993-14:2001 degradation test was used as a parameter.

Degradation tests for bioceramics should be performed in an environment which mimics *in vivo* conditions. Knowing that macrophages and osteoclasts, present at the bone repair site, excretes lactic acid in amounts which can lower the local pH to 4, the media chosen to conduce the degradation *in vitro* test had its pH lowered to 4 by adding lactic acid.

The samples were prepared using the ratio of 0.25 g of β-TCP, β-TCMP or BCMP powder per 5 ml of test solution (pH 4). Three samples of each β-TCP, β-TCMP and BCMP powders were exposed to the buffer solution for 24, 48 and 78 h with the temperature maintained at 37 °C ± 1 °C. After the exposure, the solutions were filtered and the Ca and Mg release were evaluated in a StarDust MC15 automated photometer (Diasys, Diagnostic Systems International, Holzheim, Germany).

4.2.4- INK COMPOSITION

In order to prepare the β-TCP ink, approximately, 64 g of β-TCP powder (obtained from composition A after calcination at 950 °C) were added into a 250 ml mixing cup (Thinky Inc., Japan) with 30 g of 1 mm round zirconia milling media (Union Process, Akron, Ohio), 16 g of double distilled water and 1 g of dispersant (Darvan® 821A, R.T. Vanderbilt Company, Inc., Norwalk, CT). The container was placed in a non-contact planetary mixer (model AR-250, Thinky Inc., Tokyo, Japan) for 3 minutes at 2000 rpm. Then, 4.8 g of hydroxypropyl methylcellulose (Methocel F4M, Dow Chemical Company, Midland, MI) stock solution (5 % by weight in water) was added and the suspension was mixed for additional 30 seconds at 2000 rpm. The cellulose acted as a thickening agent, which increased the suspension viscosity. Lastly, the suspension was gelled by adding, approximately, 1 g of poly(ethyleneimine) (PEI) (ICN Biomedical, Aurora, OH), as a flocculant agent, and mixed for 30 seconds at 2000 rpm. Then PEI was added in a drop-wise, followed by spinning for 30 seconds, until reaching a tooth paste consistency. Qualitatively, this tooth paste consistency is achieved when you get a stiff peak once a spatula is pulled straight up out of the ink. The figure 4.2 reveals the consistency achieved for the β-TCMP ink, which was similar to both β-TCP and BCMP ink consistency.

β-TCMP and BCMP ink formulation were adapted from the β-TCP ink formulation after some trials and errors, since they requested more water to achieve the same rheology of the β-TCP ink. The same protocol was followed for the β-TCMP and BCMP inks, but the amount of components were the following: 1 g of Darvan; 28 g of Double distilled water for the β-TCMP and 30 g for the BCMP; 65 g of β-TCMP or BCMP; 7 g of F4M; and 2 g of PEI. The β-TCP, β-TCMP and BCMP ink formulation can be found in Table 4.2.

Figure 4.2: β-TCMP ink consistence. Notice the stiff peak formed once a spatula is pulled straight up out of the ink.

Table 4.2: β-TCP, β-TCMP and BCMP inks compositions.

	β-TCP ink	**β-TCMP ink**	**BCMP ink**
Dispersant (g)	1	1	1
Double distilled water (g)	16	28	30
β-TCP powder (g)	64	-	-
β-TCMP powder (g)	-	65	-
BCMP powder (g)	-	-	65
F4M (g)	4.8	7	7
PEI (g)	1	2	2

4.2.5- ROBOTIC DEPOSITION

3D periodic scaffolds (8 mm diameter and 8 mm height) of β-TCP, β-TCMP, and BCMP, with fully interconnected porous network, were built using a robotic deposition device (Aerotech 3200, Stillwater, OK), shown in Figure 4.3, at the Department of Biomaterials and Biomimetics (NYUCD) facilities. This device had an x, y and z axis independently controlled by a custom-designed computer program (RoboCAD Beta, Stillwater, OK, USA), where the scaffold pattern was defined.

The scaffold design was create using the RoboCAD Special Shapes tool following these parameters: lattice builder; round lattice; radius 4; z spacing- 0.259 mm; n layer- 20 (number of layers); n perimeter- 2 (number of external rings surrounding the lattice pattern); Dx and Dy- 0.9 (distance between the center of the rods). Figure 4.4 shows the final design where a raster (lead in) was added to the first layer and a polyline was added to the last one. The raster was built with the aim of releasing the air encapsulated into the syringe tip and, consequently, avoiding voids entrapment into the scaffolds rods. The polyline role is to lead the syringe tip away from the scaffold structure, preventing eventual damages to the structure.

After outlining the scaffold design, the specific ink was placed in a syringe, as shown in Figure 4.5, which as positioned at the z-stage of the robocasting machine. The ink was deposited layer-by-layer (in a total of 20 layers) through a 23 GA (0.33 mm) dispense tip (Precision Tips, Nordson EFD, East Providence, RI) at a volumetric flow rate required to maintain a constant x–y printing speed. To promote an intimate contact between the layers a z spacing of 0.259 mm was used. The deposition was performed in a non-wetting oil bath to prevent non-uniform drying during the direct-write assembly, as shown in Figure 4.6.

The resulting scaffolds were dried in air at room temperature for 24 h and then placed in a high temperature furnace (Thermolyne 46100, Branstead, Dubuque, IA) kept at 400 °C for 1h, to eliminate organics, and sintered at 1100 °C during 4h (heating rate 5 °C/min).

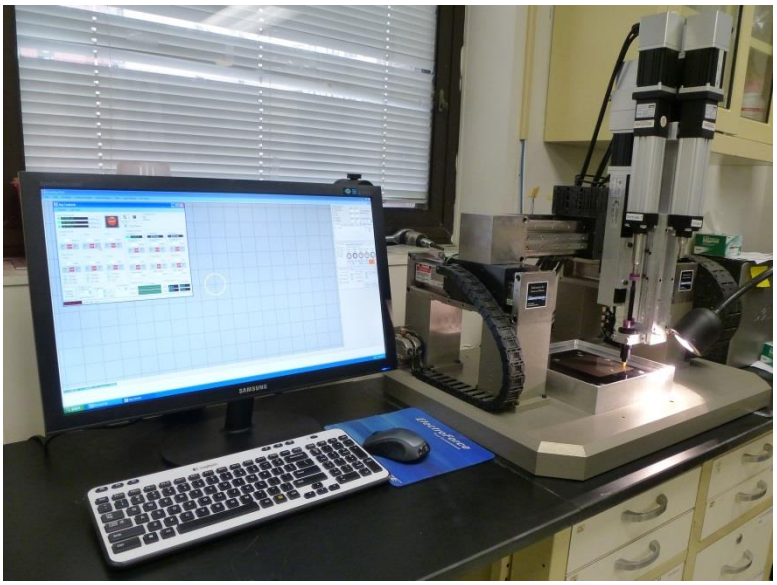

Figure 4.3: Robotic deposition device Aerotech 3200.

Figure 4.4: Scaffold design including the raster connected to the first layer and the polyline at the last one.

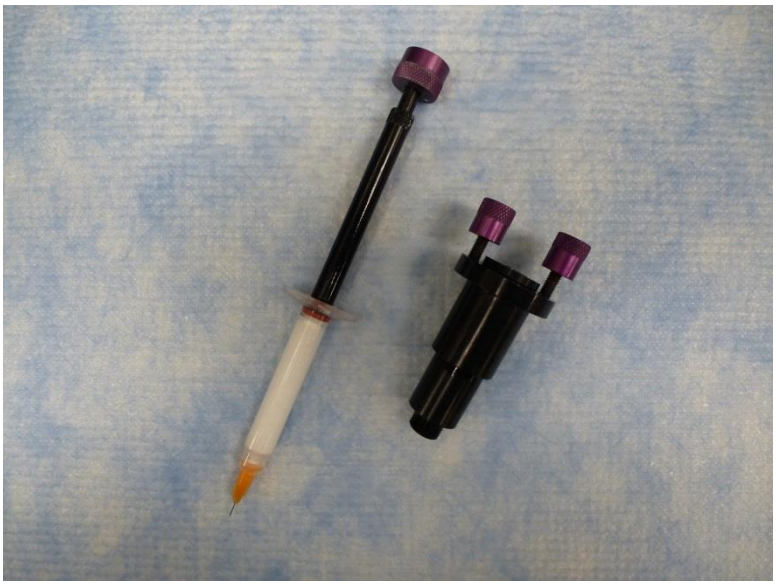

Figure 4.5: Ink placed into the robocasting system syringe. The ink placed in the syringe is the BCMP one.

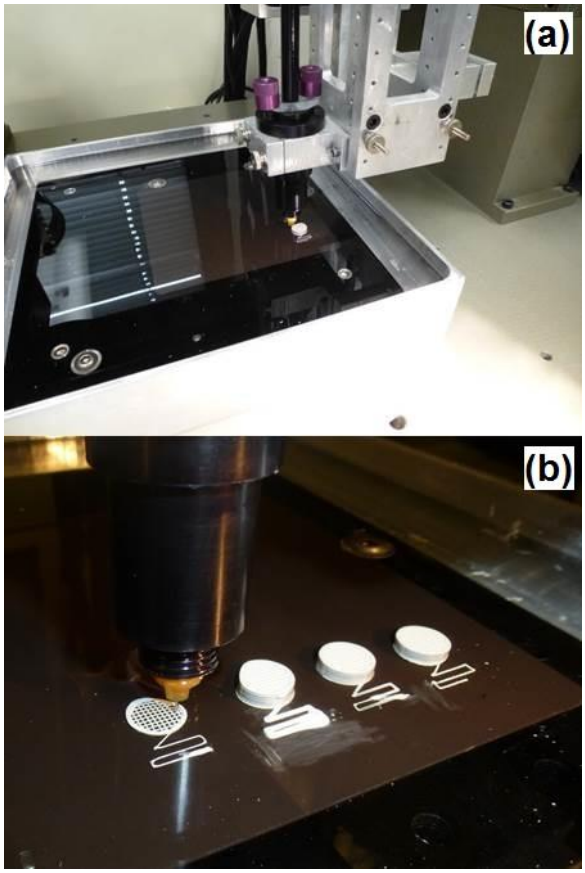

Figure 4.6: (a) direct-write assembly of a BCMP scaffold performed in a non-wetting oil bath; (b) close-up image of the ink deposition.

4.2.6- SCAFFOLDS CHARACTERIZATION

4.2.6.1- X-RAY DIFFRACTION

The β-TCP, β-TCMP and BCMP sintered scaffolds were ground into fine powders, with an agate mortar and pestle, and characterized by XRD using the same parameters applied for the green and calcined powders.

4.2.6.2- ARCHIMEDES' METHOD

The bulk density and the apparent porosity of the scaffolds were measured by the Archimedes' method. This method states that if a structure is completely or partially immersed in a fluid (gas or liquid) at rest, it will be pushed upwards by a buoyant force. The magnitude of this force is equivalent to the weight of the fluid displaced either by the volume of an object fully immersed, or by the fraction of the volume below the surface if the object is partially submerged in the fluid (ZOU *et al.*, 1997).

In order to determine the density, the samples were dried in a furnace overnight at 120 °C. A hydrostatic scale was used to obtain the true and apparent mass of the scaffolds.

The density of the specimens was determined with equation (4.1):

$$Density(g/cm3) = \frac{W_{dry} \times \rho_{water}}{(W_{dry} - W_{wet})} \qquad (4.1)$$

where W_{dry} is the weight corresponding to the dry scaffold, W_{wet} is the weight corresponding to the scaffold soaked in water and $\rho water$, the density of water (0,99705 g/cm^3) at 25 °C.

The porosity of a scaffold is given by the ratio between the real volume and the volume of voids (Karageorgiou and Kaplan, 2005). It was possible to measure the real volume of the porous scaffolds (V_{real}) using Equation 4.2:

$$V_{real} = \frac{\pi d^2}{4} \times h \qquad (4.2)$$

where π is approximately equal to 3.14159 and d and h are the scaffold diameter and height respectively.

To measure the voids volume (V_{voids}) was used equation 4.3:

$$V_{voids} = V_{real} \times \frac{W_{dry}}{density} \qquad (4.3)$$

The apparent porosity of the scaffolds was determined according to equation 4:

$$Porosity = \left(\frac{V_{voids}}{V}\right) X\ 100\% \quad (4.4)$$

4.2.6.3- SCANNING ELECTRON MICROSCOPE

The macro and microstructural morphology of the sintered scaffolds were obtained by SEM (JEOL, JSM6460LV) working at 15 kV. The samples were mounted on aluminum stubs with carbon tape, sputtered-coated with a thin gold layer (Emitech, K550, USA) to avoid electrical charging.

4.2.6.4- MICRO COMPUTED TOMOGRAPHY (MICRO-CT)

The micro-CT physical principle consists on the attenuation of X-rays during their interaction with an object. One scaffold of each β-TCP, β-TCMP and BCMP group

were analyzed in a high energy microtomography system (Skyscan/Bruker, model 1173) at Nuclear Instrumentation Laboratory/Engineering Nuclear Program from Federal University of Rio de Janeiro, Brazil. In order to obtain the micro-CT images, each scaffold was placed in the experimental equipment inside an acrylic cylinder, with compatible dimension, to ensure that the sample was not going to move during the entire acquisition process.

The system was calibrated to operate at 70 kV of energy and a current of 114 μA. Additionally, one aluminum filter (1.0 mm thickness) was used in order to reduce the contribution of low energy photons, which cause beam hardening effect. The samples were scanned with 7.08 μm pixel size and a flat panel detector was employed with a 2240 x 2240 pixels matrix.

After the acquisition process, the software Nrecon® (Nrecon 2011- version 1.6.8.0) and InstaRecon (InstaRecon 2011- version 1.3.9.2) were used to rebuild the X-ray images. Some parameters were modified in order to create a better image during the reconstruction, e.g., Gaussian smoothing filters with degree 3, a ring artifact reduction with level 13 and a beam hardening artifact correction with a degree of 25% were used.

CTAn ® (CTAn 2012) (v.1.13.2.0) software was used with the aim of processing and analyzing the images. The quantified parameters were the total volume of the binary-converted objects (root canal and pores) within the volume of interest, VOI, (bone volume, BV, mm^3). All the objects within the region of interest (ROI) were analyzed. The Kuwahara filter, which is a nonlinear filter that reduces image noise and also preserves the border information, was used after the segmentation procedure. In this study a global threshold (TH) was used for the accuracy of the quantification process, considering a gap of 0 to 255 (VIANNA *et al.*, 2013 and OLIVEIRA *et al.*, 2012). By using the TH, it was possible to separate the object (white) from the empty space (black). The parameters were quantified directly in 3D based on a model of the surface volume extracted. Moreover, all objects, in the selected region, were analyzed together and the combined results were calculated as the total volume of the samples.

4.2.6.5- MECHANICAL COMPRESSION TEST

A universal testing machine (Instron Series 5566, USA), equipped with a 10 KN load cell, was used for the uniaxial compression test. The crosshead speed was set at 0.5 mm/min, and 15 specimens of each group were tested, with the purpose of getting statistically reliable values, according to the ASTM C773 – 88 (Standard Test Method for Compressive (Crushing) Strength of Fired Whiteware Materials) referred on the ASTM F2883-11 (Standard Guide for Characterization of Ceramic and Mineral Based Scaffolds used for Tissue-Engineered Medical Products (TEMPs) and as Device for Surgical Implant Applications). The specimens were cylinders with 8 mm diameter and 5 mm height.

Statistical analysis of the mechanical compression data were performed by one-way ANOVA at 95.0 % confidence interval using the software Origin 8.0 (OriginLab Corporation, USA). Multiple comparisons between groups were performed by the Tukey's test.

CHAPTER 5

RESULTS AND DISCUSSION

5.1- CALCIUM PHOSPHATES POWDERS CHARACTERIZATION

Figure 5.1(a) shows the XRD patterns of β-TCP, β-TCMP (Mg-substituted TCP) and BCMP (Mg-substituted biphasic calcium phosphate) powders obtained after calcining the CDA's powders. Approximately 90 g of β-TCP (JCPDS 09-0169) were obtained after calcining Mg-free CDA, while 90 g of β-TCMP and BCMP powders were obtained after calcining Mg-substituted CDA's prepared with different Mg/Ca molar ratio and pH. The BCMP pattern confirmed, besides β-TCMP, the presence of HA (JCPDS 09-0432) in the biphasic powder. As shown in Figure 5.1(b), the β-TCMP (JPDS 13-0404) spectrum is shifted to the right compared to the β-TCP; which indicates the Mg substitution in the β-TCMP powder. Therefore, hydrolysis method may be a promising alternative route for synthesizing calcium phosphates powders such as β-TCP, β-TCMP and BCMP. It offers a less technical-sensitive processing route compared to the precipitation method, where a close control of the pH is requested during the first three hours of the synthesis. Moreover, a bigger amount of powder can be obtained through the hydrolysis synthesis compared to the precipitation synthesis.

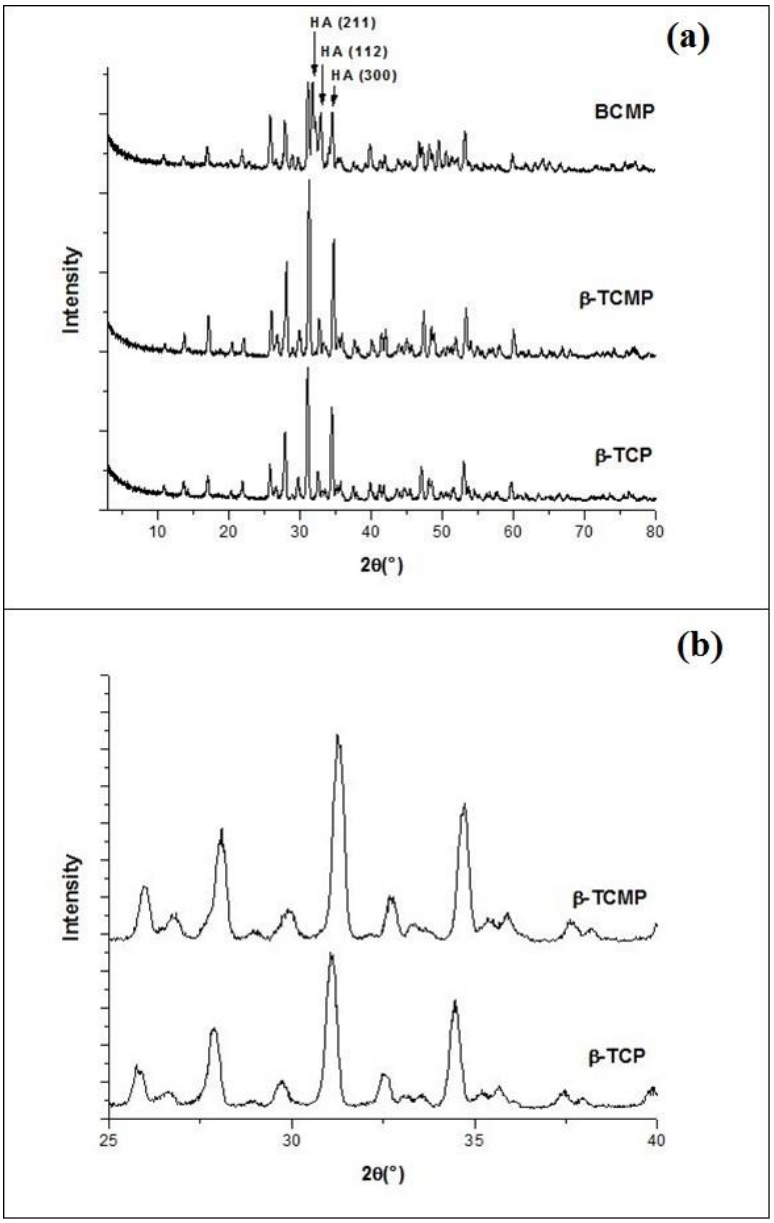

Figure 5.1: a) XRD spectra of β-TCP, β-TCMP and BCMP powders. The BCMP spectrum confirms the intimate mixture of β-TCMP and HA (JCPDS 9-0432); b) notice that the β-TCMP spectrum is shifted to the right comparing to the β-TCP spectrum, which indicates Mg-for-Ca substitution.

After calcining the CDA at 950 °C the HA/β-TCMP ratio was 51/49 (Figure 5.2). The method (precipitation, hydrolysis or mechanical mixture), pH and temperature employed in the synthesis of the unsintered apatite have intimate relation with calcium deficiency (Ca/P molar ratio < 1.67). In its turn, the calcium deficiency determines the

HA/β-TCP ratio in the BCP, which determines its reactivity. In other words: the lower the ratio, the higher the reactivity (DACULSI *et al.*, 2003).

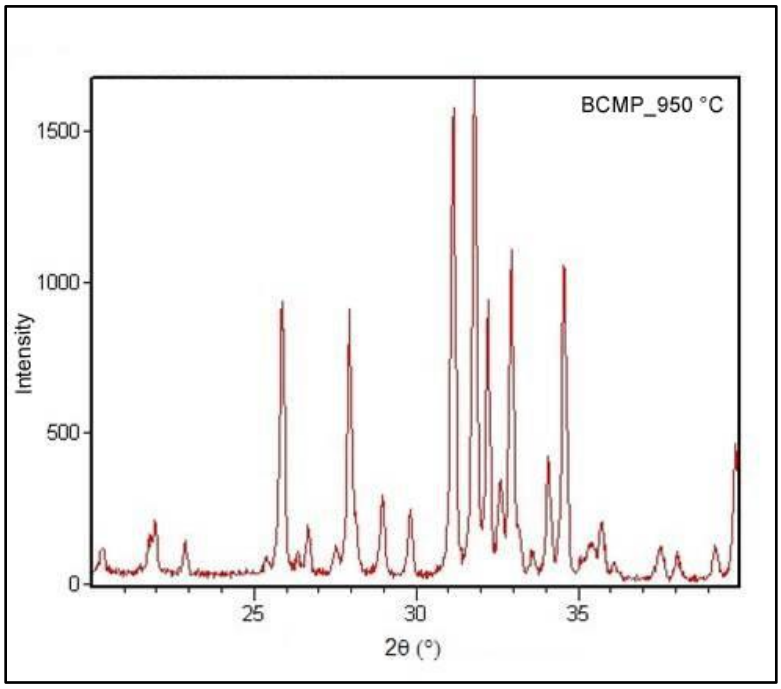

Figure 5.2: XRD spectrum displaying the HA/β-TCMP ratio (51/49) of the BCMP powder calcined at 950°C.

The Mg/Ca molar ratio, obtained by ICP, was 0.11 and 0.04 for the β-TCMP and BCMP samples, respectively. The β-TCP presented a 0.01 Mg/Ca molar ratio; this could be associated with the fact that some manufactures use magnesium to stabilize DCPD (brushite) against transformation to DCPA (monetite) since it partially converts to DCPA in dry storage (LEGEROS, 1991). Moreover, the (Ca+Mg)/P ratio was 1.47 for the β-TCMP, while the theoretical Ca/P ratio for TCP is 1.5 (DESTAINVILLE *et al.*, 2003) and 1.62 for the BCMP samples. The Ca/P, Mg/Ca, Ca+Mg/P molar ratios of the β-TCP, β-TCMP and BCMP calcined powders can be observed in Table 5.1. RAYNAUD *et al.*, 2002, showed that CDA powders with 1.5 < Ca/P < 1.667 had dissociated into a mixture of HA and β-TCP. In their paper, as the temperature increased from 700 °C to 1100 °C the ratio HA/β-TCP was smaller. The same behavior was observed in our study.

Table 5.1: Ca/P, Mg/Ca, Ca+Mg/P molar ratios of the β-TCP, β-TCMP and BCMP calcined powders.

	Ca/P	Mg/Ca	Ca+Mg/P
β-TCP	1.38	0.01	1.39
β-TCMP	1.33	0.11	1.47
BCMP	1.56	0.04	1.62

The FTIR spectra, Fig. 5.3, of the calcined powders showed absorption bands characteristic of tricalcium phosphate (947, 974, and 1120 cm^{-1}) and pyrophosphate (727 and 1200 cm^{-1}) for the β-TCP samples. The presence of pyrophosphate may be explained by the fact that the Ca/P ratio of the calcined β-TCP samples was 1.38. The theoretical Ca/P ratio for TCP is 1.5; therefore, for a Ca/P ratio < 1.5, pyrophosphate was expected (DESTAINVILLE *et al.*, 2003). However, the XRD didn't identify any pyrophosphate phase (JCPDS 09-0346) for the β-TCP, possibly because that phase was present in a non-detectable amount. β-TCP as well as absorption band associated to HA (OH^-, 630 cm^{-1}) were detected in the BCMP samples.

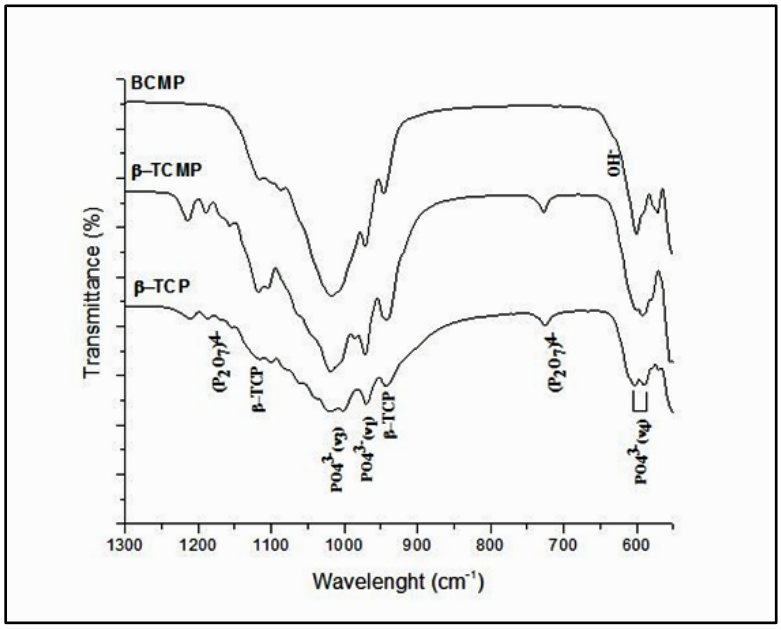

Figure 5.3: FTIR spectra of the CDAs powders and after transformation to β-TCP, β-TCMP and BCMP by calcination at 950°C.

Particle size and distribution analyses showed that the β-TCP, β-TCMP and BCMP powders had particles ranging from 0.18 - 79.43 μm, 0.27 - 138.04 μm and 0.18 - 45.71 μm, respectively. Correspondingly, 29.6, 53.8 and 49.3 % of the particles were in the range of 2 and 14 μm for the β-TCP, β-TCMP and BCMP groups. Approximately 10 % of the β-TCP, β-TCMP and 6.5 % of the BCMP particles were under 2 μm. As shown in Figure 5.4: the BCMP powder presented a unimodal particle size distribution, where the bigger volume of particles is in the range of 18.02± 0.30 μm; the β-TCP powder reveals a multimodal distribution, where the granulometric distribution includes three ranges (2.38 - 16.60 μm; 6.97 - 88.67 μm and 0 - 64,85 μm) and there were three groups that included the bigger volume of particles for each range(9.54 ± 5.78 μm; 47.65 ± 3.39 μm and 28.78 ± 0.70 μm, see Figure 5.5 for deconvoluted curves); the β-TCMP powder also presents a multimodal distribution, where the granulometric distribution includes three ranges (0 - 69.18 μm; 0 -30.2 μm and 79.43 – 158.48 μm, see Figure 5.6 for deconvoluted curves) and there were three groups that included the bigger volume of particles for each group: 40.09 ± 1,47 μm, 15,46 ± 0,37 μm and 100.68 ± 0.56 μm.

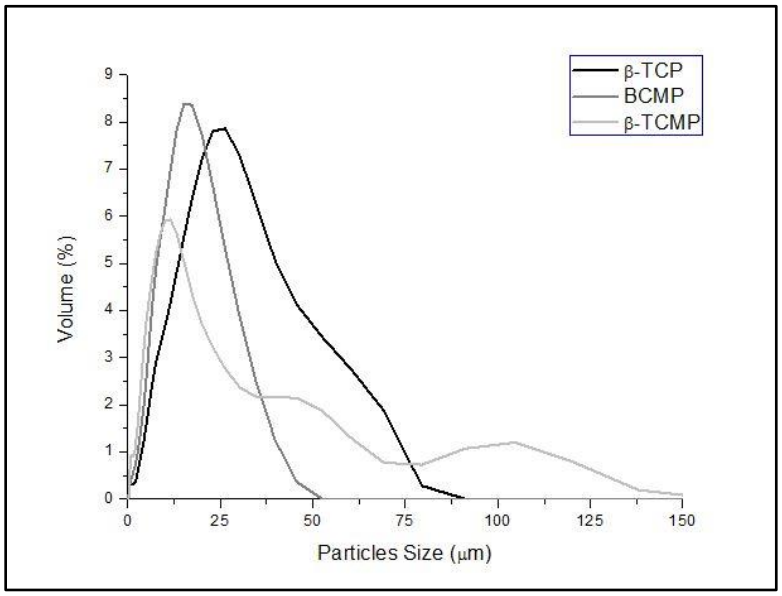

Figure 5.4: Particle size and distribution of β-TCP, β-TCMP and BCMP powders.

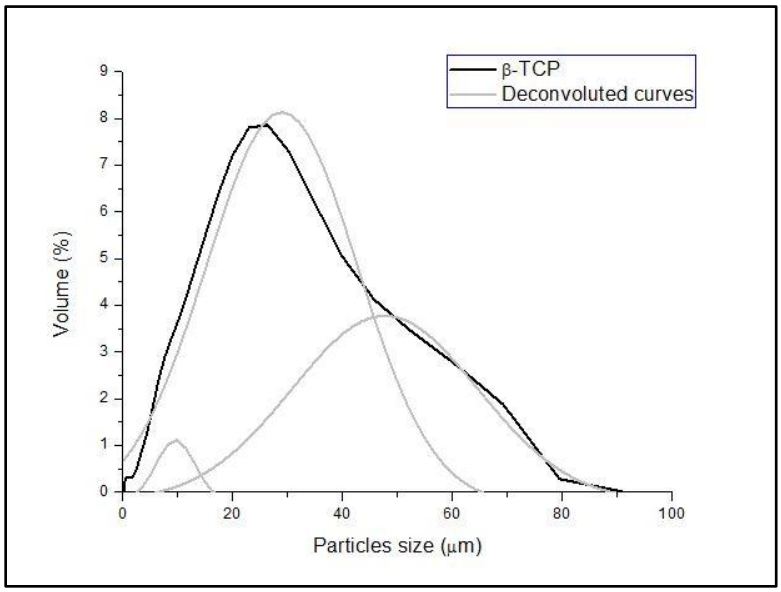

Figure 5.5: β-TCP particle size and distribution and respective deconvoluted curves.

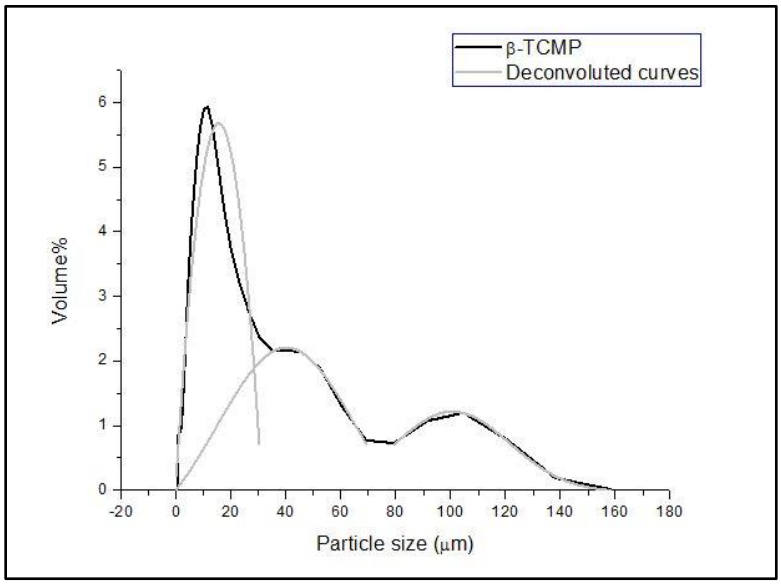

Figure 5.6: β-TCMP particle size and distribution and respective deconvoluted curves.

Figure 5.7 shows SEM micrographs of the calcium phosphates (CaP) powders after calcination at 950 °C for 11 h. The morphology and size of calcined powders showed to be suitable for 3D printing purposes because the powders obtained consisted of small and dense round particles. According to MIRANDA *et al.*, 2006, micrometer order particle

size, spherical and smooth surfaces are ideal features for starting powders used in inks for robotic deposition.

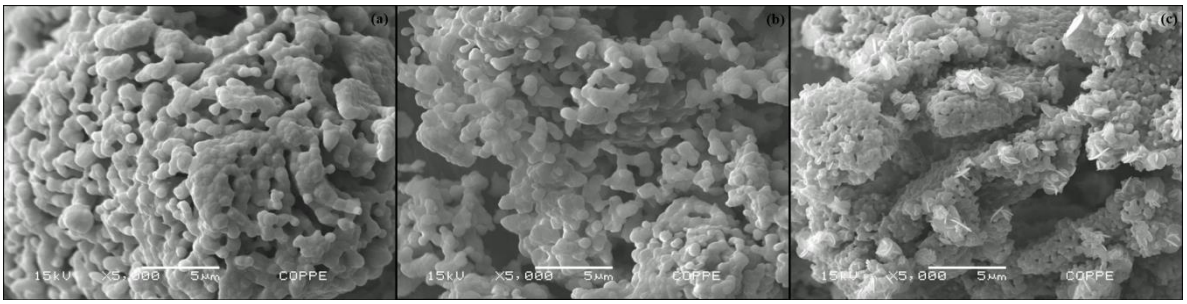

Figure 5.7: SEM micrographs of β-TCP (a); β-TCMP (b); and BCMP (c) powders obtained by calcination, at 950 ˚C, of three different CDAs composition.

In this study, the MTT assay performed on MC3T3-E1 cells , Fig. 5.8, indicated that the β-TCP, β-TCMP and BCMP powders, obtained by hydrolysis, promoted cell proliferation, indicating non-toxicity for this particular cell line.

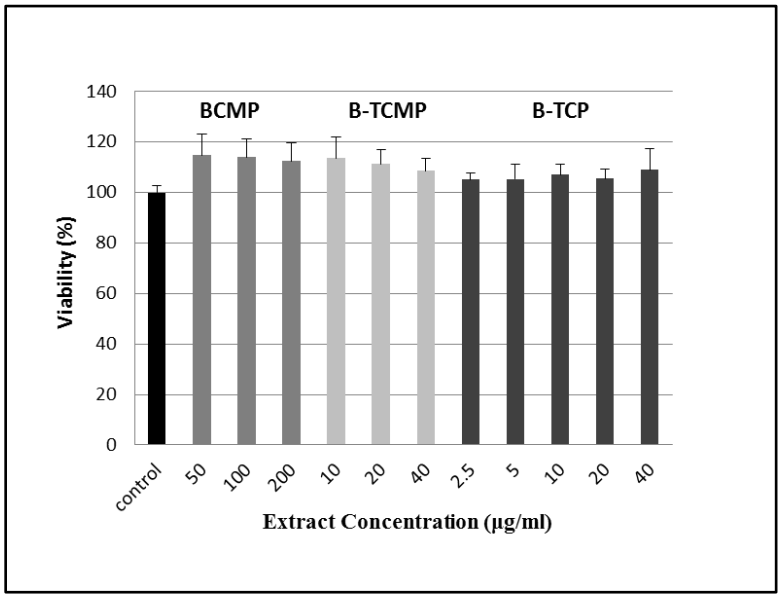

Figure 5.8: Cell viability assay performed on MC3T3-E1 cells.

Mineralization assay results indicated that the degradation products of the β-TCP, β-TCMP and BCMP are conductive to bone formation. The amount of mineralized nodules was higher in the β-TCP sample, followed by β-TCMP and BCMP samples as revealed in Figure 5.9. Bone formation markers (ALP and osteocalcin) and bone resorption markers (TGF- β and collagen) activity in MC3T3-E1 cell line had a higher expression for β-TCP group, followed by β-TCMP and BCMP group, as shown on Fig. 5.10. This behavior can be explained for the fact that the presence of Mg ions retards the dissolution of CaP (BOSE *et al.*, 2011) due to increase of structural stability (ARAÚJO *et al.*, 2009; BANDYOPADHYAY *et al.*, 2006 and SCOTT *et al.*, 2011). The reason why Mg stabilizes the structure of TCP may reside in the fact that Mg atoms are located closer to the axis of the cluster than the Ca atoms, due to their smaller ionic radius (BANDYOPADHYAY *et al.*, 2006). Yassuda *et al.* (2013) showed, in their *in vivo* study, that β-TCP granules had a positive influence on osteoclast activity compared to β-TCMP granules. This could be related to the fact that the faster β-TCP degradation rate, in comparison to β-TCMP, induces a faster bone ingrowth.

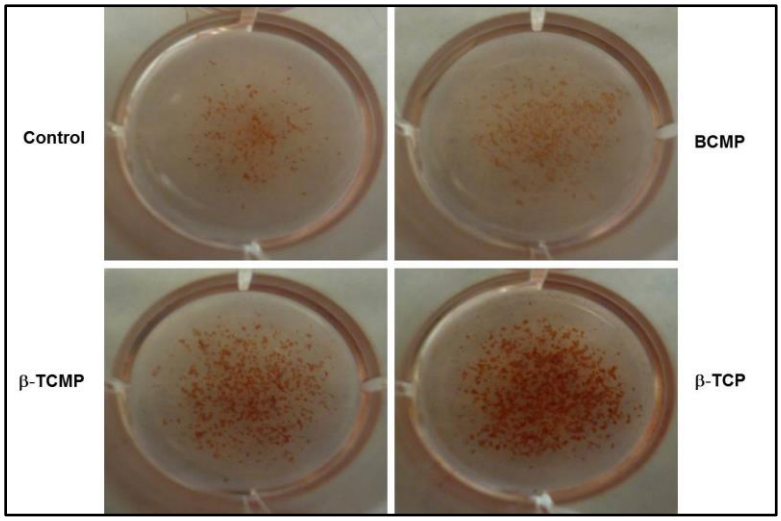

Figure 5.9: Mineralization assay results showing the mineralized nodules, which are degradation products of the β-TCP, β-TCMP and BCMP powders.

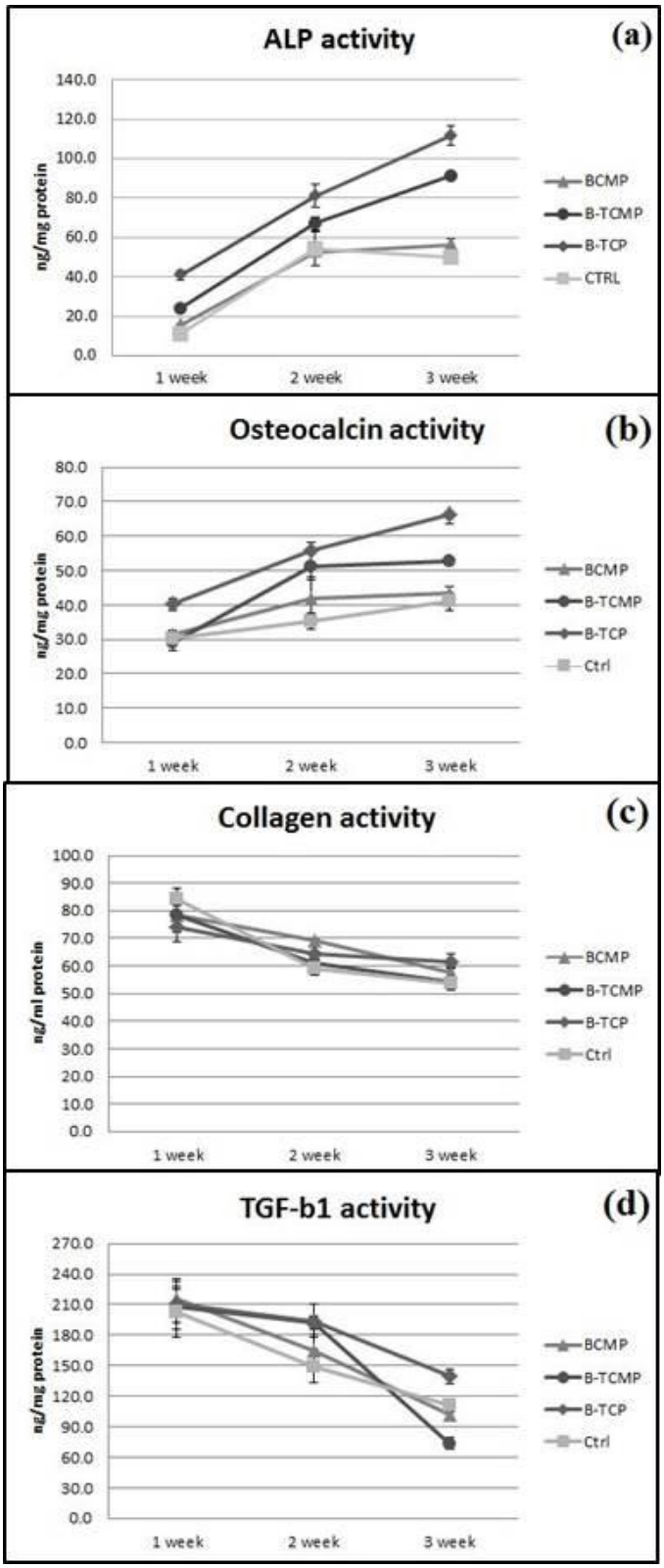

Figure 5.10: Expression of bone formation markers (a and b) and bone resorption markers (c and d) for all calcined powders.

The degradation test results revealed that the Ca release was bigger on β-TCP samples than on β-TCMP and BCMP samples (Figure 5.11). This is in agreement with the literature, where TCP is more soluble than HA; and, as discussed before, Mg substitutions in TCP and BCP increase crystal stability, which reduces the Ca release (BOSE *et al.*, 2011, GARRIDO *et al.*, 2011, and LEGEROS, 1991). According to Mg release results, the BCMP and β-TCMP samples had similar results (Figure 5.12). Knowing that a ceramic with solubility rate closer to the bone formation rate has a better the influence on bone tissue growth (CONZ *et al.*, 2005); and both β-TCMP and BCMP had their structures stabilized by Mg, extending their dissolution, it can be stated that these results are in accordance with the mineralization and ELISA results.

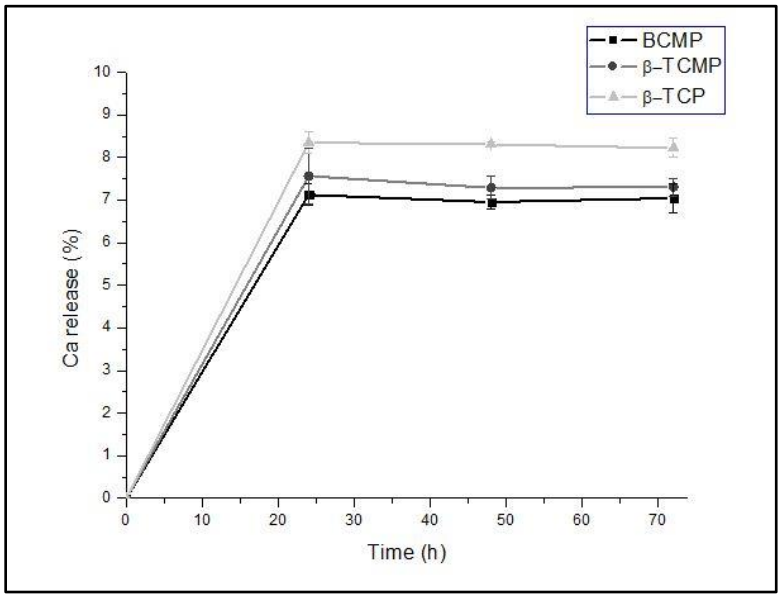

Figure 5.11: β-TCP, β-TCMP and BCMP calcium release.

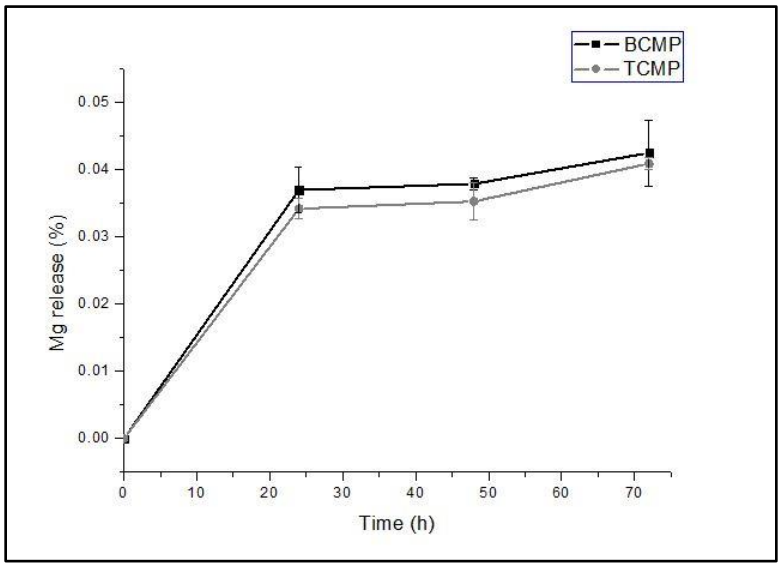

Figure 5.12: β-TCMP and BCMP magnesium release.

5.2- SCAFFOLDS CHARACTERIZATION

The 3D structures obtained from the β-TCP, β-TCMP and BCMP inks were cylinders (**Φ =** 8 mm x H = 5 mm) composed of 20 layers, with two perimeter rims surrounding a parallel array of rods (0.33 mm) with an inter-rod spacing of, approximately, 500 μm. The layers were rotated 90˚ with respect to each other to give raise to an interconnected structure. Figure 5.13 reveals the macrostructure of a sintered β-TCMP scaffold. Figure 5.14 shows a photomicrograph which exhibit details about the macro and microstructure of a β-TCP sintered scaffold. Similar images were registered from the β-TCMP and BCMP scaffolds macrostructure.

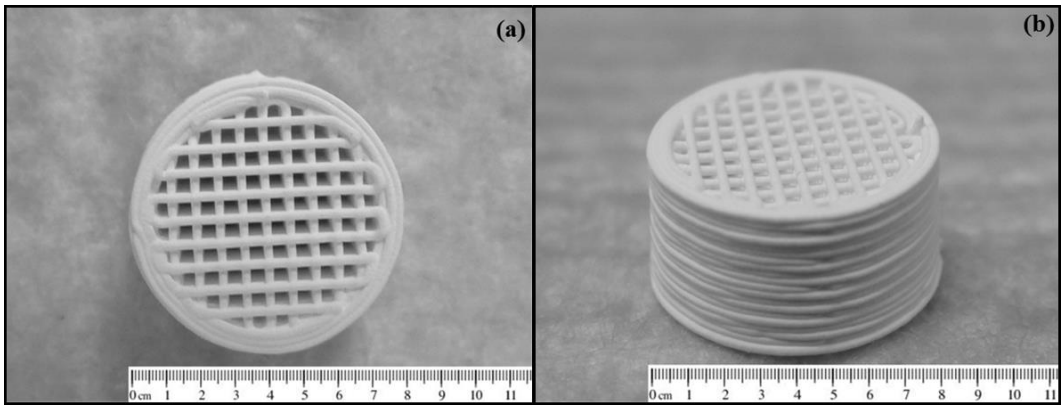

Figure 5.13: Macrostructure of sintered β-TCMP scaffold: (a) top view; (b) lateral view.

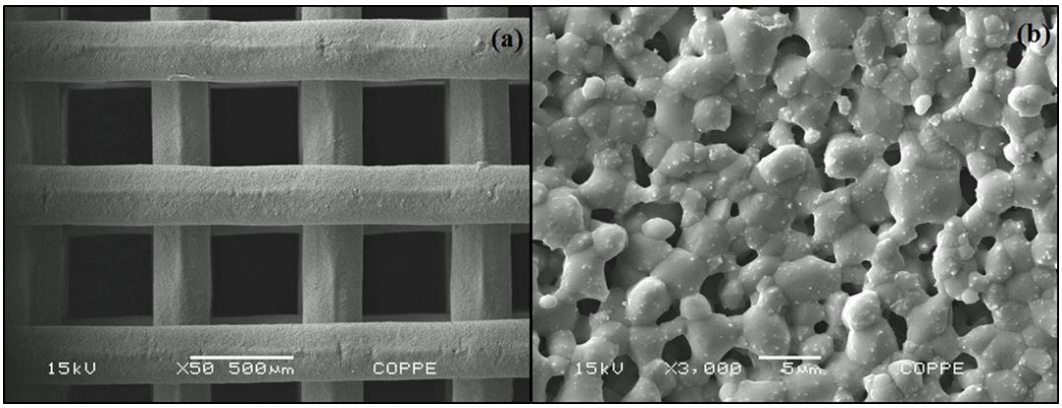

Figure 5.14: SEM images of sintered scaffold with different magnifications. The image corresponds to the β-TCP scaffold and it's possible to observe the macroporosity (a) and microporosity (b) associated with robocasting method.

The scaffolds built in this study reproduced, in their architecture, the typical thicknesses of the trabeculae, which are in the range of 100 to 300 µm, and typical intertrabecular spacing, which is in the order of 500 to 1500 µm (KEAVENY *et al.*, 2004). This was confirmed by micro-CT trabecular thickness distribution and trabecular separation distribution morphometric parameters analyses displayed on Figures 5.15 and 5.16, respectively. Many studies have stated that an optimal scaffold for bone replacement should have a 3D geometry similar of that of the ingrowing trabecular bone, because it may be an effective approach for fast and efficient conduction of new bone across

significant distances in these osteoconductive structures (MATHIEU *et al.*, 2006, SIMON et al., 2007, SIMON et al., 2008).The importance of the pore size and architecture for a scaffold relies on the fact that they are essential for controlling metabolic aspects such as the diffusion of oxygen, growth factors, and nutrients to the cells (SIMON *et al.*, 2003).

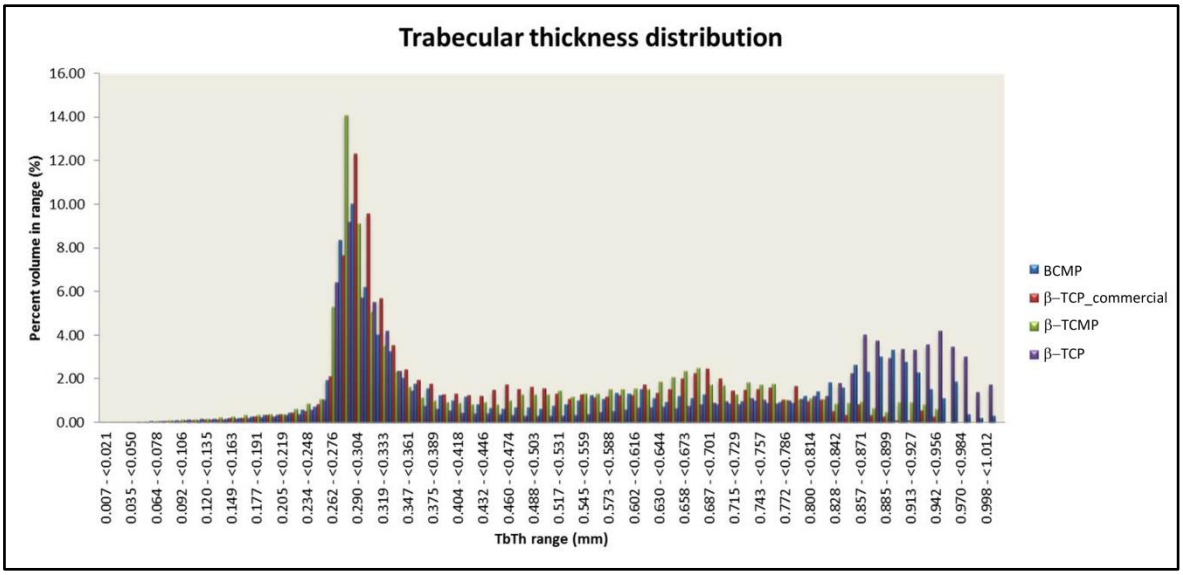

Figure 5.15: Micro-CT trabecular thickness distribution morphometric parameters analyses.

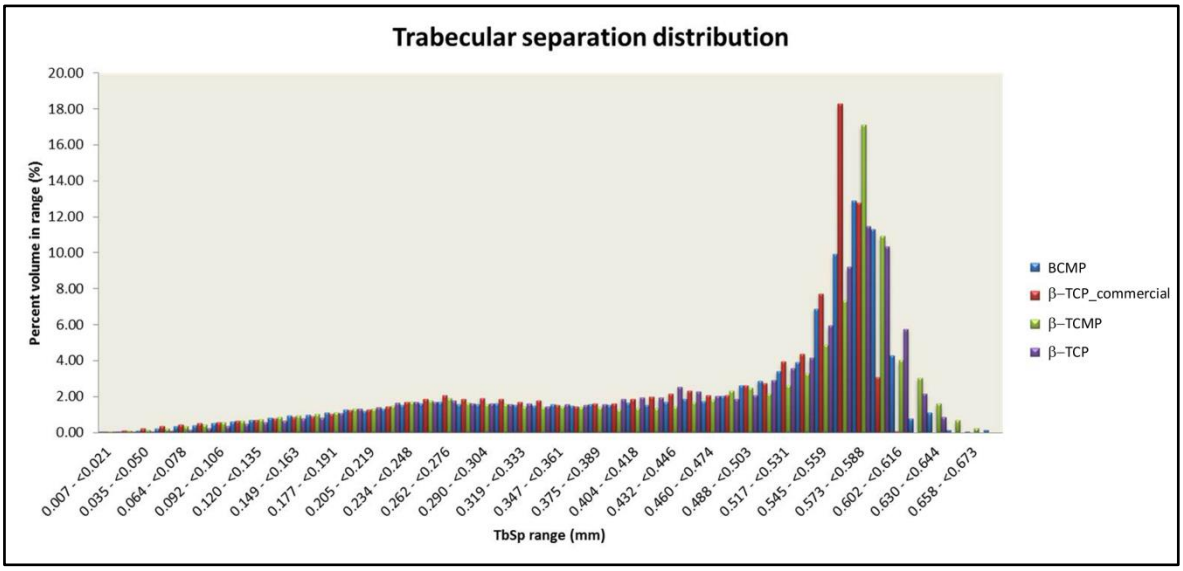

Figure 5.16: Micro-CT trabecular separation distribution morphometric parameters analyses.

The micro-CT 3D reconstruction revealed that the scaffolds had an interconnected macroporous network, as show in Figure 5.17. The performance of a 3D bone scaffold is not only related to the biomaterial selection, but also to its architecture and consequent interaction with the surrounding tissue. In order to be considered properly designed, a scaffold should allow bone ingrowth and provide vascularization for the new tissue. This can be achieved by controlling the scaffold pore volume fraction, pore interconnections, and pore size. It's known that a highly interconnected porosity volume fraction provides a large surface area, which facilitates cells to migrate, proliferate, and differentiate (ROY *et al.*, 2003, TAMPIERI *et al.*, 2001). However, high volume fraction is usually associated with low mechanical properties, which is also a requisite to these types of scaffold.

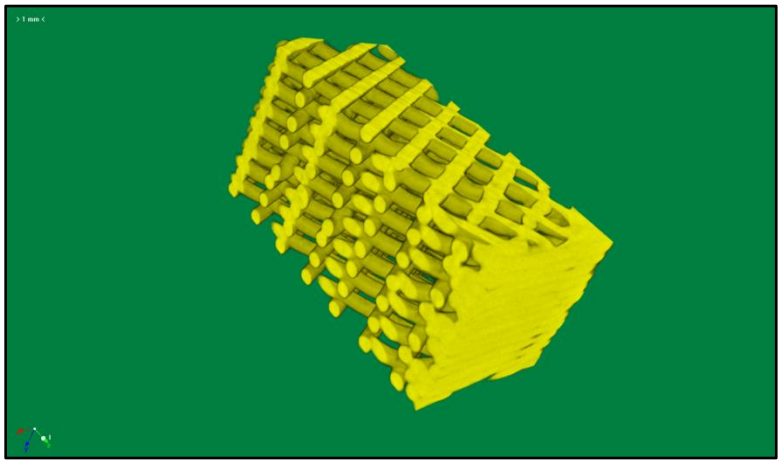

Figure 5.17: Micro-CT image reconstruction, showing the interconnected macroporous network of the BCMP scaffold.

The Archimedes' method results had shown a higher apparent density for the β-TCP group (6,400 ± 0,109 g/cm^3) followed by the β-TCMP (4,922 ± 0,142 g/cm^3) and BCMP (4,628 ± 0,092 g/cm^3) groups; and a smaller open porosity fraction for the β-TCP group (0,319 ± 0,067) compared to the β-TCMP (0,453 ± 0,005) and BCMP (0,481 ± 0,013) groups . The difference between the three densities was expected as the packing densities of the colloidal suspensions can be affected by the liquid-to-powder ratio (BAROUD, *et al.*, 2005) and the amount of dispersant employed (KRISHNA *et al.*, 2006). Additionally, an increase of the viscosity in tooth-paste-like suspensions, containing

calcium phosphates, is observed with a decrease of the particle size (BAROUD, *et al.*, 2005). As the BCMP powder had smaller particle followed by the β-TCMP and β-TCP, the amount of water employed to achieve similar viscosity between the three inks was bigger in the BCMP composition.

The compressive stress-strain curve for β-TCMP specimen 6 showed on Figure 5.18 reveals a linear-elastic regime which ends when the rods begin to collapse. As the compressive collapse progress, a horizontal plateau can be observed on the stress-strain curve. Finally, when the opposing rods touch each other, the stress rises before the failure (GIBSON E ASHBY, 1997, GIBSON *et al*., 2010).

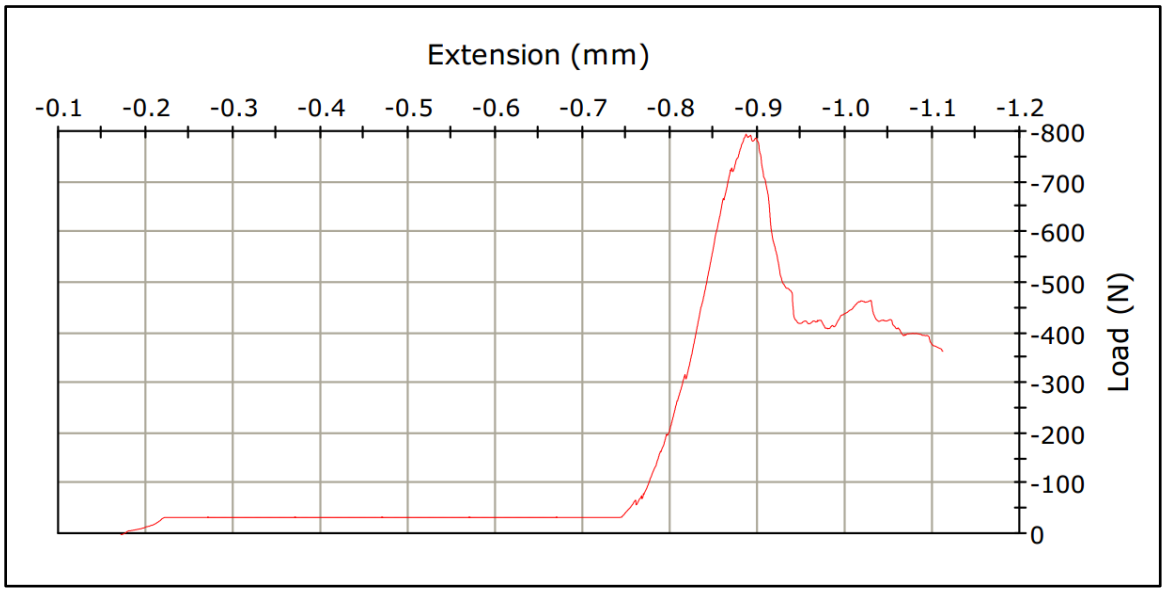

Figure 18: Compressive stress-strain curve for β-TCMP specimen 6.

Studies with trabecular bone have been registered a wide variation of strength which is usually in the range of 4 to 12 MPa (JOHNSON & HERSCHLER, 2011, HOUMARD *et al.*, 2013 and HUTMACHER *et al.* 2007). A graph with the uniaxial compression strength values for the β-TCP, β-TCMP and BCMP scaffolds can be observed in Figure 5.19.

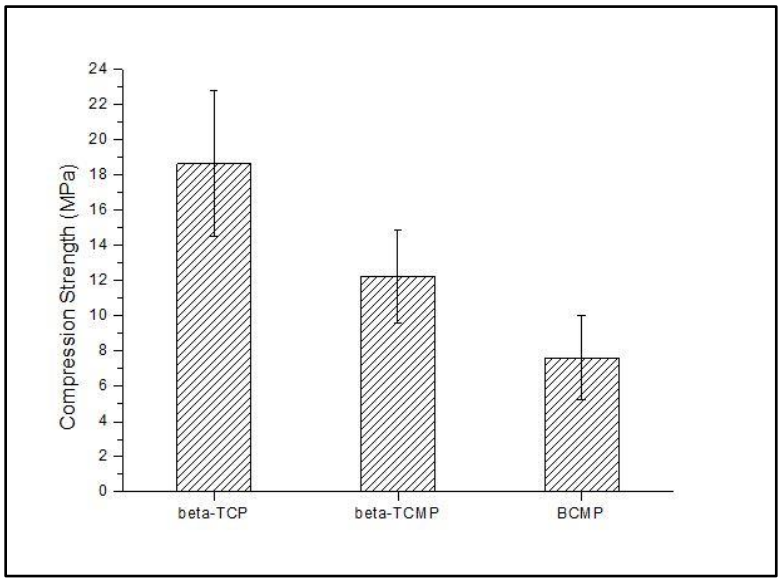

Figure 5.19: Compression strength values for the β-TCP, β-TCMP and BCMP scaffolds (n=15).

The mean compressive strength values of β-TCP, β-TCMP and BCMP scaffolds (n=15) were 18.7 (± 4.14), 12.2 (± 2.67) and 7.60 (± 2.36) MPa, and the maximum compressive strength values were 26.6, 15.8 and 10.6 MPa, respectively. Those scaffolds could be applied for reconstructing low loading bearing defects such as maxillofacial ones. The goal would be to treat the defect with a scaffold that reproduces the shape of the patient's bone defect, improving the bone re-growth.

The mechanical test results were statistically significant for the 3 groups. Even though β-TCP group achieved better mechanical behavior compared to β-TCMP and BCMP groups, we can't associate the better mechanical properties exclusively to the β-TCP powder performance, since the inks produced for the different groups had distinct solid/liquid ratios. Studies based on statistical analysis of data available in the literature indicated that compressive strength is proportional to density squared (GIBSON *et al*., 2010). Therefore the density of the scaffolds may have influenced the mechanical compression results. Beyond that, adding more water to the β-TCMP and BCMP ink composition was necessary to adjust the ink rheology since Mg ions extend the dissolution behavior of calcium phosphates (BOSE et al., 2011; LEGEROS, 1991; LI et al., 2009 and YASSUDA et al., 2013). Furthermore, the better mechanical behavior of β-TCMP in comparison with the BCMP scaffolds could be a result of better particle packing, since the

β-TCMP powder had a multimodal distribution whereas the BCMP powder had a unimodal one. Finally, another factor that may have influenced the poorest mechanical performance of the BCMP scaffolds was the partial transformation of HA after the scaffold sintering process. A XRD analyses revealed that the HA/β-TCMP ratio changed from 51/49 (calcined powder) to 27/73 after the sintering process of the scaffold at 1100 °C for 4 h, as shown in Figure 5.20.

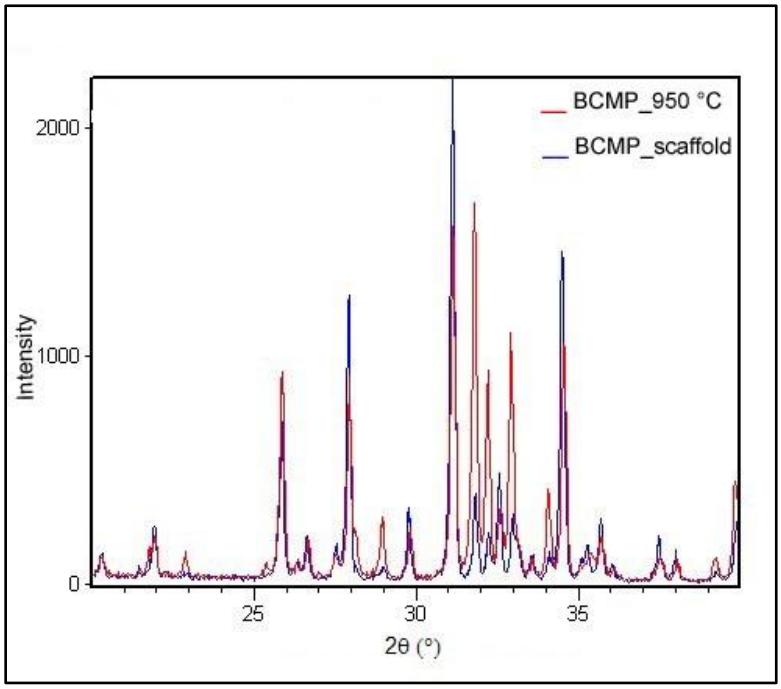

Figure 5.20: Combined XRD spectra of BCMP powder calcined at 950 °C (HA/β-TCMP ratio= 51/49) and BCMP scaffold sintered at 1100°C (HA/β-TCMP ratio= 27/73).

Chapter 6

6.1- CONCLUSIONS

Based on the analyses of the results, the following conclusions were established:

- Calcium phosphate powders as: β-TCP; β-TCMP; and BCMP were successfully produced via hydrolysis of different CDA's, followed by calcination at 950 °C for 11 h.
- According to a 24 h MTT assay, the β-TCP; β-TCMP; and BCMP powders induced MC3T3-E1 cells proliferation, which indicated non-toxicity for this particular cell line.
- Mineralization assay and bone markers activity suggested that all the powders present potential value in bone tissue engineering as they are likely to promote bone mineralization.
- The powders particle size, ranging from 0.18 to 138.04 μm, and shape were suitable for developing inks for use in a robocasting machine (Aerotech 3200, Stillwater, OK). However, differences in particle size and distribution led to distinct liquid/powder ratio for the β-TCP; β-TCMP; and BCMP inks.
- Periodic cylindrical bone scaffolds (**Φ =** 8mm x H = 5mm) with interconnected pores of order of 460 μm were obtained by robocasting.
- The mean compression strength of the sintered scaffolds varied from 7.6 to 18.7MPa and was compatible or even superior (β-TCP group) to trabecular bone compression strength values (2 to 12 MPa).

6.2- SUGGESTED IMPROVEMENTS FOR FUTURE WORKS

- The particle size and distribution should be better controlled in order to achieve uniformity among the groups;
- Rheology analyses should be performed for the different inks obtained;
- *In vivo* tests should be performed.

REFERENCES

ARAÚJO, J.C., SADER, M.S., MOREIRA, E.L., MORAES, V.C.A., LEGEROS, R.Z., SOARES, G.A., 2009. “Maximum substitution of magnesium for calcium sites in Mg-β-TCP structure determined by X-ray powder diffraction with the Rietveld refinement” ***Materials Chemistry and Physics,*** v.118, n. 2-3 (Dec), pp. 337-340.

ASTM C773 - 88 Standard Test Method for Compressive (Crushing) Strength of Fired Whiteware Materials.

ASTM F2883 - 11 Standard Guide for Characterization of Ceramic and Mineral Based Scaffolds used for Tissue-Engineered Medical Products (TEMPs) and as Device for Surgical Implant Applications.

BABIS, G.C., SOUCACOS, P.N., 2005. “Bone scaffolds: the role of mechanical stabillity and instrumentation” ***Injury***, v. 36, n. 4 (Nov), pp. S38-S44.

BANDYOPADHYAY, A., BERNARD, S., WIECHANG, X., BOSE, S., 2006. “Calcium phosphate-based resorbable ceramics: influence of MgO, ZnO, and SiO2 dopants” ***J A Ceram Soc***., v. 89, n. 9 (Sept), pp. 2675-2688.

BAROUD, G., CAYER, E., BOHNER, M., 2005. “Rheological characterization of concentrated aqueous β-tricalcium phosphate suspensions: The effect of liquid-to-powder ratio, milling time, and additives” ***Acta Biomaterialia***, v. 1, n.3 (May), pp. 357-363.

BOANINI, E., GAZZANO, M., BIGI, A., 2010. “Ionic substitutions in calcium phosphates synthesized at low temperature” ***Acta Biomaterialia***, v. 6, n.6 (June), pp. 1882-1894.

BOSE, S., TARAFDER, S., BANERJEE, S.S., DAVIES, N.M., BANDYOPADHYAY, A., 2011. “Understanding in vivo response and mechanical property variation in MgO, SrO and SiO2 doped β-TCP” ***Bone***, v. 48, n. 6 (June), pp. 1282–1290.

BUTSCHER, A., BOHNER, M., HOFMANN, S., GAUCKLER, L., MÜLLER, R., 2011. “Structural and material approaches to bone tissue engineering in powder-based three-dimensional printing” ***Acta Biomaterialia***, v.7, n. 3 (Mar), pp. 907–920.

CONZ, M.B., GRANJEIRO, J.M., SOARES, G.A., 2005. “Physocochemical characterization of six commercial hydroxyapatites for medical dental applications as bone graft” ***J Appl Oral Sci***, v. 13, n. 2 (June), pp. 136-40.

DACULSI, G., LABOUX, O., MALARD, O., WEISS, P., 2003. “Current state of the art of biphasic calcium phosphate bioceramics” ***Journal of Materials Science: Materials in Medicine***, v. 14, n.3 (March), pp. 195-200.

DESTAINVILLE A, CHAMPION E, BERNACHE-ASSOLLANT D, LABORDE E., 2003. “Synthesis, characterization and thermal behavior of apatitic tricalcium phosphate” ***Materials Chemistry and Physics***, v. 80, n. 1 (April), pp. 269–277.

DETSCH, R., SCHAEFER, S., DEISINGER, U., ZIEGLER, G., SEITZ, H., LEUKERS, B., 2011. "In vitro-osteoclastic activity studies on surfaces of 3D printed calcium phosphate scaffolds". ***Journal of Biomaterials appplications***, v. 26, n. 3 (Sep), pp. 359-380.

DOBLARÉ, M., GARCÍA, J.M., GÓMEZ, M.J., 2004. “Modelling bone tissue fracture and healing: a review” ***Engineering Fracture Mechanics***, v. 71, pp.1809–1840.

DOROZHKIN, S.V., 2009. “Calcium Orthophosphates in Nature, Biology and Medicine” ***Materials***, v. 2, n. 2 (April) pp. 399-498.

EIJKEN, M., 2007, *Human Osteoblast Differentiation and Bone Formation: Growth Factors, Hormones and Regulatory Networks.* Ph.D. dissertation, Department of Internal Medicine of the Erasmus MC, Rotterdam, Netherlands.

GARRIDO, C.A., LOBO, S.E., TURÍBIO, F.M., LEGEROS, R.Z., 2011. “Biphasic Calcium Phosphate Bioceramics for Orthopaedic Reconstructions: Clinical Outcomes” ***International Journal of Biomaterials***, v. 2011, pp. 1-9.

GIBSON, L.J., ASHBY, M.F. 1997. "Cancellous bone". In: D.R., Suresh, S., Ward, I.M. Clarke (eds). ***Cellular solids/ Structure and properties***. 2 ed., chapter 11, Cambridge, Cambridge University Press.

GIBSON, L.J., ASHBY, M.F., HARLEY, B.A. 2010. ***Cellular Materials in nature and medicine***. 1 ed. New York, Cambridge University Press.

HORNER, E.A. *et al*., 2010. “Long Bone Defect Models for Tissue Engineering Applications: Criteria for Choice” ***Tissue Engineering: Part B.***, v. 16, n. 2 (April), pp. 263-271.

HOUMARD, M., FU, Q., GENET, M., SAIZ, E., TOMSIA, A.P., 2013. “On the structural, mechanical, and biodegradation properties of HA/β-TCP robocast scaffolds” ***J Biomed Mater Res Part B***. v. 101, n. 7(Oct), pp. 1233–1242.

HUTMACHER, D., 2000. "Scaffolds in tissue engineering bone and cartilage". ***Biomaterials***, v. 21, n. 24 (Dec), pp. 2529-2543.

HUTMACHER, D.W., SCHANTZ, J.T., LAM, C.X.F., TAN, K.C., LIM, T.C., 2007. “State of the art and future directions of scaffold-based bone engineering from a biomaterials perspective” ***J Tissue Eng Regen Med***, v.1, n4 (Jul-Aug), pp. 245–60.

ISO 10993-14:2001- Biological evaluation of medical devices Part 14: Identification and quantification of degradation products from ceramics.

JOHNSON, A. J. W., HERSCHLER, B. A., 2011. "A review of the mechanical behavior of CaP and CaP/polymer composites for applications in bone replacement and repair". ***Acta Biomaterialia****,* 2011, v. 7, n. 1 (Jan), pp. 16-30.

JUNQUEIRA, L.C., CARNEIRO, J. 2010. "Tecido Ósseo". ***Histologia Básica****.* 10 ed., chapter 8, Rio de Janeiro, Guanabara-Koogan.

KARAGEORGIOU, V., KAPLAN, D., 2005 “Porosity of 3D biomaterial scaffolds and osteogenesis” ***Biomaterials***, v. 26, n. 27 (Sept), pp. 5474–5491.

KEAVENY, T.M., MORGAN, E.F., YEH, O.C., 2004. ***Standard Handbook of biomedical engineering and design***. New York, The McGraw-Hill Companies.

KRISHNA PRASAD P.S.R., VENUMADHAV REDDY A., RAJESH P.K., PONNAMBALAM P., PRAKASAN K., 2006. “Studies on rheology of ceramic inks and spread of ink droplets for direct ceramic ink jet printing” ***Journal of Materials Processing Technology***, v.176, n. 1-3 (June), pp. 222–229.

LANGER, R., VACANTI, J.P. 1993. “Tissue Engineering” ***Science****, v.* 260, n. 5110 (May), pp. 920-926.

Langer, R., Vacanti, J.P., 1993. “Tissue Engineering” ***Science***, v. 260, n. 14 (May), pp. 920-926.

LEE, D., KUMTA, P.N., 2010. “Chemical synthesis and stabilization of magnesium substituted brushite” ***Materials Science and Engineering C***, v. 30, n. 7 (Aug), pp. 934-943.

LEGEROS, R.Z., 1991. “Calcium Phosphates in Oral Biology and Medicine”. 1 ed., Basel, Switzerland, S. Karger.

LEGEROS, R.Z., 2008. “Calcium Phosphate-Based Osteoinductive Materials” ***Chem. Rev.***, v. 108, n. 11 (Nov), pp. 4742–4753.

LEGEROS, R.Z., LIN, S., ROHANIZADEH, R., MIJARES, D., LEGEROS, J.P., 2003. “Biphasic calcium phosphate bioceramics: preparation, properties and applications” ***Journal of Material Science: Materials in Medicine***, v. 14, n. 3 (March), pp. 201-209.

LI, J., ZHANG, L., LV, S., LI, S., WANG, N., ZHANG, Z., 2011. “Fabrication of individual scaffolds based on a patient-specific alveolar bone defect model” ***Journal of Biotechnology***, v. 151, n. 1 (Jan), pp. 87–93.

LI, X., ITO, A., SOGO, Y., WANG, X., LEGEROS, R.Z., 2009. “Solubility of Mg-containing β-tricalcium phosphate at 25 °C”. ***Acta Biomaterialia***, v.5, n. 1 (Jan), pp. 508-517.

MATHIEU, L.M, MUELLER, T.L., BOURBAN, P.E., PIOLETTI, D.P., MÜLLER, R., MÅNSON, J.A.E., 2006. “Architecture and properties of anisotropic polymer composite scaffolds for bone tissue engineering” ***Biomaterials***, v. 27, n. 6 (Feb), pp. 905–916.

MICHNA, S., WU, W., LEWIS, J.A. 2005. “Concetrated hydroxyapatite inks for direct-write assembly of 3-D periodic scaffolds”. ***Biomaterials***, v. 26, n. 28 (Oct), pp. 5632-5639.

MIRANDA, P., PAJARES, A., SAIZ, E., TOMSIA, A.P., GUIBERTEAU, F. 2007a. “Fracture modes under uniaxial compression in hydroxyapatite scaffolds fabricated by robocasting” ***J Biomed Mater Res A.***, v. 83, n.3 (Dec), pp. 646-655.

MIRANDA, P., PAJARES, A., SAIZ, E., TOMSIA, A.P., GUIBERTEAU, F., 2007b. “Mechanical properties of calcium phosphate scaffolds fabricated by robocasting” ***J Biomed Mater Res A.***, v. 85, n. 1 (April) pp. 220-227.

MIRANDA, P., SAIZ, E., GRYN, K. TOMSIA, A.P. 2006. “Sintering and robocasting of B-tricalcium phosphate scaffolds for orthopaedic applications”. ***Acta* Biomaterialia**, v. 2, n. 4 (Jul), pp. 457-466.

MIRANDA, P., SAIZ, E., GRYN, K., TOMSIA, A.P., 2006. “Sintering and robocasting of β-tricalcium phosphate scaffolds for orthopedic applications” **Acta Biomaterialia**, v. 2, n.4 (Jul), pp. 457–466.

NAKASE, T., YOSHIKAWA, H., 2006. “Potential roles of bone morphogenetic proteins (BMPs) in skeletal repair and regeneration” ***J Bone Miner Metab***, v.24, n. 6, pp. 425–433.

OLIVEIRA, M.F.S., LIMA, I., BORGHI, L., LOPES, R.T., 2012. “X-ray microtomography application in pore space reservoir rock” ***Applied Radiation and Isotopes***, v. 70, n. 7 (Jul), pp. 1376-1383.

Qu, S.X., Guo, X., Weng, J., Cheng, J.C.Y., Feng, B., Yeung, H.Y., Zhang, X.D., 2004. “Evaluation of the expression of collagen type I in porous calcium phosphate ceramics implanted in an extra-osseous site” ***Biomaterials***, v. 25, n. 4 (Feb) pp. 659–667.

RAYNAUD, S., CHAMPION, E., BERNACHE-ASSOLLANT, D., THOMAS, P., 2002. “Calcium phosphate apatites with variable Ca/P atomic ratio I: Synthesis, characterisation and thermal stability of powders” ***Biomaterials***, v. 23, n. 4 (Feb), pp. 1065-1072.

RICHARD, R.C., SADER, M.S., DAI. J., THIRÉ, R.M., SOARES, G.D., 2013. “Beta-type calcium phosphates with and without magnesium: From hydrolysis of brushite powder to robocasting of periodic scaffolds” ***J Biomed Mater Res A.***, DOI: 10.1002/jbm.a.35040.

ROY, T.D., SIMON, J.L., RICCI, J.L., REKOW, E.D., THOMPSON, V.P., 2003. “Performance of hydroxyapatite bone repair scaffolds created via three-dimensional fabrication techniques”. ***J Biomed Mater Res A.***, v. 67, n. 4 (Dec), pp. 1228-1237.

SADER, M.S., LEGEROS, R.Z., SOARES, G.A., 2009. “Human osteoblasts adhesion and proliferation on magnesium-substituted tricalcium phosphate dense tablets”. ***J Mater Sci: Mater Med***, v. 20, n. 2 (Feb), pp. 521-527.

SADER, M.S., LEWIS, K., SOARES, G.A., LEGEROS, R.Z., 2013. “Simultaneous Incorporation of Magnesium and Carbonate in Apatite: Effect on Physico-chemical Properties” ***Materials Research***, v. 16, n. 4 (Jul-Aug), pp. 779-784.

SCHELLER, E.L., KREBSBACH, P.H., KOHN, D.H., 2009. “Tissue engineering: state of the art in oral rehabilitation” ***Journal of Oral Rehabilitation***, v. 36, n. 5 (May), pp. 368–389.

SCOTT, P.R., CROW, J.A., LEGEROS, R.Z., KRUGER, M.B., 2011. “A pressure-induced amorphous phase transition in magnesium-substituted β-tricalcium phosphate” ***Solid State Communications***, v. 151, n. 21, pp. 1609-1611.

SIMON, J.L., MICHNA, S., LEWIS, J.A., REKOW, E. D., THOMPSON, V.P., SMAY, J.E., YAMPOLSKY, A., PARSONS, J.R., RICCI, J.L., 2007. “In vivo bone response to 3D periodic hydroxyapatite scaffolds assembled by direct ink writing” ***J Biomed Mater Res A.***, v. 83, n. 3 (Dec), pp. 747–758.

SIMON, J.L., REKOW, E. D., THOMPSON, V.P., BEAM, H., RICCI, J.L., PARSONS, J.R., 2008. “MicroCT analysis of hydroxyapatite bone repair scaffolds created via three-dimensional printing for evaluating the effects of scaffold architecture on bone ingrowth” ***J Biomed Mater Res A.***, v.85, n. 2 (May), pp. 371–377.

SIMON, J.L., ROY, T.D., PARSONS, J.R., REKOW, E.D., THOMPSON, V.P., KEMNITZER, J., RICCI, J.L., 2003. “Engineered cellular response to scaffold architecture in a rabbit trephine defect” ***J Biomed Mater Res A.***, v. 66, n. 2 (Aug), pp. 275-82.

SMAY, J.E., CESARANO III, J., LEWIS, J.A. 2002b. “Colloidal inks for directed assembly of 3-D periodic structures” ***Langmuir,*** v. 18, n.14, pp. 5429-5437.

SMAY, J.E., GRATSON, G.M., SHEPHERD,R.F., CESARANO III,J., LEWIS,J.A. 2002a. “Directed Colloidal Assembly of 3D Periodic structures” ***Advanced Materials***, v. 14, n. 18 (Sept), pp. 1279-1283.

TADIC, D., EPPLE, M., 2004. “A thorough physicochemical characterisation of 14 calcium phosphate-based bone substitution materials in comparison to natural bone” ***Biomaterials***, v. 25, n. 6 (Mar), pp. 987–994.

TAMINI, F., LE NIHOUANNEN, D., BASSET, D.C., *et al*., 2011. “Biocompatibility of magnesium phosphate minerals and their stability under physiological conditions” ***Acta Biomaterialia***, v. 7, n.6 (Jun), pp. 2678-2685.

TAMPIERI, A., CELOTTI, G., SPRIO, S., DELCOGLIANO, A., FRANZESE, S., 2001. “Porosity-graded hydroxyapatite ceramics to replace natural bone” ***Biomaterials***, v. 22, n.11 (Jun), pp. 1365–1370.

UCHIDA, T., IKEDA, S., OURA, H., TADA, M., NAKANO, T., FUKUDA, T., MATSUDA, T., NEGORO, M., ARAI, F. 2008. “Development of biodegradable scaffolds based on patient-specific arterial configuration” ***J. Biotechnol.***, v. 133, n. 2 (Jan), pp. 213–218.

VIANNA, V.F., BONFIM, D.C., CAVALCANTI, A.S., FERNANDES, M.C., KAHN, S.A., CASADO, P.L., LIMA, I.C., MURRAY, S.S., MURRAY, E.J.B., DUARTE, M.E.L., 2013. “Late adherent human bone marrow stromal cells form bone and restore the hematopoietic microenvironment *in vivo”* ***BioMed Research International*** v. 2013, March, pp.1-11.

XIE, B., PARKHILL, R.L., WARREN, W.L., SMAY, J.E., 2006. “Direct writing of three-dimensional polymer scaffolds using colloidal gels”. ***Advanced Functional Materials***, v. 16, n.13 (Sept), pp. 1685-1693.

YASSUDA, D.H., COSTA, N.F.M., FERNANDES, G.O., ALVES, G.G., GRANJEIRO, J.M., SOARES, G.D.A., 2013. “Magnesium incorporation into β-TCP reduced its in vivo resorption by decreasing parathormone production” ***J Biomed Mater Res A.***, v. 101, n. 7 (Jul), pp. 1986-93.

ZOU, L., BLOEBAUM, R.D., BACHUS, K.N., 1997. “Reproducibility of techniques using Archimedes’ principle in measuring cancellous bone volume” ***Med. Eng. Phy.***, v.19. n. 1 (Jan), pp. 63-68.